

Copyright

by

Carl Joseph Larosche

1999

**Test Method for Evaluating Corrosion Mechanisms in Standard Bridge
Columns**

by

Carl Joseph Larosche, B.S.C.E.

Thesis

Presented to the Faculty of the Graduate School

of The University of Texas at Austin

in Partial Fulfillment

of the Requirements

for the Degree of

Master of Science in Engineering

The University of Texas at Austin

August 1999

**TEST METHOD FOR EVALUATING CORROSION MECHANISMS IN
STANDARD BRIDGE COLUMNS**

APPROVED BY
SUPERVISING COMMITTEE:

John E. Breen

Michael E. Kreger

To My Parents, Wife and Children

Acknowledgements

This thesis was conducted at the Phil M. Ferguson Structural Engineering Laboratory at the University of Texas at Austin for the Texas Department of Transportation. Assistance provided by TxDOT Project Director Bryan Hodges and the TxDOT team of BRINSAP Personnel, Brian Merrill and Randy Cox as well as financial assistance provided by TxDOT in support of Project 1405 is greatly appreciated.

I would like to thank Dr. John Breen first and foremost. Dr. Breen supported me from inception into the graduate program and guided me through completion, never once doubting me or giving up as I struggled along. A thanks also goes to Dr. Michael Kreger for his input and guidance throughout the project. Graduate study at the University of Texas at Austin was truly an honor for me.

I would like to thank the Doctoral Candidate on this project, Jeff West. I am especially grateful for Jeff's willingness to go above and beyond to help me find my way with this project. Jeff's willingness to meet at anytime to discuss the project and the impact upon Jeff's time spent away from his family will be appreciated forever. Without the aid of Jeff West, I seriously doubt I would have completed this thesis. In addition, I would like to thank the rest of the group at FSEL that worked on the Project, including Brad Keoster, Diana Hun and John Riordan. Diana (Dee) and John spent long hours in the laboratory tying steel and building forms. I certainly appreciate their hard work and dedication.

This acknowledgement section would not be complete without mentioning the support I received from all of the staff at FSEL. Paramount among those, as special thanks goes to Ms. Laurie Golding for all her help in guiding me though the procurement process at the university, ordering all of the project's equipment and material and keeping me on task. In addition, thanks go to April Jenkins for helping me though the administrative process. Members of the staff in building 24 that assisted me in the project are: Blake Stasney, and Pat Ball.

The graduate school experience and the friendships made are very important to me. I'm grateful to have met Paul, "Willie", John, Chuck and the rest of the FSEL "gang". A special thanks to this entire group, the graduate years will always hold a special place in my memories.

I am also grateful to Lindsey Mijares, Jeremiah Fasl, and all the other young soccer players that taught me "real" commitment, dedication and sacrifice to obtain a goal.

Finally I would like to thank my family who supported me without question over the entire time. In addition, a special thanks to my father, Carl Larosche, who was there for all of my family from the beginning and for providing me all of the unconditional support. To my wife, my children and my father, I thank you from the bottom of my heart and I will always be grateful.

Chuck Larosche
Austin, Texas
August, 1999

Abstract

Test Method for Evaluating Corrosion Mechanisms in Standard Bridge Columns

by

Carl Joseph Larosche, M.S.E.

The University of Texas at Austin, 1999

SUPERVISOR: John E. Breen

In recent years there has been a rapid increase in usage of post-tensioned concrete in substructure elements such as bridge piers, pylons, hammerhead bents, straddle bents and other types of unusual applications. These elements, like current substructure elements in Texas, are subject to durability attack. This attack may come from exposure to aggressive environments such as de-icing salts, salt water, and sulfate-rich soils. This study involves defining the status of the current substructure systems employed in Texas and the pertinent variables involved in increasing substructure longevity with post-tensioned elements. An extensive analysis will define durability regions in Texas as these regions apply to substructures. Upon completion of this analysis, a field review was made in regions where extensive corrosive attack on columns is prevalent. This review helped identify the main variables in the corrosion attack on current Texas bridge columns. The main focus of this thesis is to accurately model the Texas bridge columns

and develop a suitable test method for determining the effects of the corrosion process on conventional and post-tensioned columns and their connections.

TABLE OF CONTENTS

Acknowledgement	v
Abstract.....	vii
List of Tables	xii
List of Figures.....	xiii
1. Introduction.....	1
1.1 General.....	1
1.2 Substructure Design and Construction	2
1.2.1 General Design Concepts for Reinforced Concrete.....	2
1.2.2 Post-Tensioned Concrete	4
1.3 Corrosion of Reinforcing Steel in Concrete	9
1.3.1 Corrosion Principles	10
1.3.2 Half-Cell Potential	12
1.3.3 Rate-of-Corrosion	15
1.4 Research Objectives	19
1.5 Scope	21
2. BRINSAP Data	22
2.0 Introduction.....	22
2.1 The Appraisal System.....	22
2.2 Initial BRINSAP Findings	25
2.3 The Geographic Regions	30
2.3.1 Replacement Costs.....	32
2.4 Field Trip Investigations.....	36
2.4.1 The Amarillo District.....	39
2.4.2 The Corpus Christi District.....	46
2.4.3 The Austin District.....	48
2.5 Future BRINSAP Studies	49

3. Test Program.....	50
3.1 Introduction.....	50
3.2 Specimen Design	50
3.2.1 Specimen Variables	51
3.2.2 Development of the Column Model	53
3.3 Materials	55
3.3.1 Concrete	55
3.3.2 Post Tension Steel.....	60
3.3.3 Reinforcing Steel	67
3.3.4 PE Duct	68
3.3.5 Galvanized Duct	70
3.3.6 Grouts.....	71
3.4 Specimen Preparation	72
3.4.1 Foundation Design.....	72
3.4.2 Foundation Reinforcement.....	80
3.4.3 Foundation and Column Formwork.....	82
3.4.4 Epoxy Connections	87
3.4.5 Concrete Casting.....	88
3.4.6 Post Tension Stressing / Grouting	93
3.5 Test Setup	96
3.5.1 Service Load Applications.....	96
3.5.2 Irrigation System.....	101
3.6 Test Procedure	104
3.6.1 Half-cell Potential Measurements.....	106
3.6.2 Chloride Powder Measurements	108
3.6.2.1 Method of Calibration.....	108
3.6.2.2 Silver Nitrate Titration.....	109
4. Results and Discussion	112

4.1 Introduction.....	112
4.2 Active Specimens.....	113
4.3 Connection Comparisons	114
4.4 Effects of The Concrete	115
4.5 Effects of PT Protection.....	115
4.6 Effects of Duct Material	115
5. Summary, Conclusions and Recommendations.....	117
Appendix A- Preliminary Half-Cell Readings for Column Specimens.....	119
Appendix B-Listing of On-System Bridges in Texas with a Substructure Rating of 5 or Below.....	130
Appendix C-Long Term Corrosion Tests on Column Specimens: Supplementary Material.....	197
Bibliography	205
Vita	208

List of Tables

Table 1.1 Index Numbers for The National Bridge Inventory Rating System.....	5
Table 1.2-Breakdown of the Deficient Structures Nationally	6
Table 1.3-Standard EMF Series	12
Table 2.1-The Rating Guide for BRINSAP Appraisal (TxDOT).....	24
Table 2.2-Pertinent Variables in On-System Bridges with a Substructure Rating of 5 or below	26
Table 2.3-Durability Regions and Their Respective Districts.....	31
Table 2.4-A Summary of BRINSAP Data	34
Table 2.5-Additional Districts and Their Adverse Conditions.....	38
Table 2.6- Districts and Their Respective Regions	38
Table 2.7-Approximate Year Built of Sample in Amarillo	39
Table 2.8-Individual Projects Reviewed in the Amarillo District	40
Table 2.9-Chloride Powder Test on Columns, Project 275-1-38 Amarillo (IH 40).....	45
Table 3.1-Chloride Ion Penetration Based on Charge Passed.....	57
Table 3.2- Local TxDOT Class C Mix Designs Tested for Permeability By AASHTO 277.....	58
Table 3.3-Results of AASHTO Permeability Tests	60
Table 3.4-Matrix Combination of Duct and P/T Bars	69
Table 3.5-Compressive Strength Values for Columns 1,3,4,6 & 8.....	90
Table 3.6 Compressive Strength Values for Columns 2,5,7,9 7 10	91
Table 3.7-The Concrete Batch Designs for Concrete Closure Casting	92
Table 3.8-Field Calculations for the P/T Stressing of the Columns	94
Table 3.9-The Column Specimens under Service Load.....	97
Table 3.10-Procedure for Chloride Analysis.....	108
Table 3.11-Procedure for Silver Nitrate Titration.....	109
Table 3.12-Examples of Determination of Titration Endpoint.....	110
Table 4.1-Summary of the Ten Specimens Probability of Corrosion	113

List of Figures

Figure 1.1-Post-tensioning Schematic.....	7
Figure 1.2-Copper and Zinc with their Ions at Equilibrium.....	10
Figure 1.3-Reversible Copper Electrode.....	11
Figure 1.4-Polarization Diagram for Reinforced Concrete.....	17
Figure 2.1-The State of Texas, by District Depicting Mean Age of Deficient Bridge Structures.....	28
Figure 2.2-Average ADT by District.....	35
Figure 2.3 –Average Number of Spans per Bridge.....	37
Figure 2.4- Top and Side Splitting of Upper Reinforcement in a Bent Cap (Amarillo).....	41
Figure 2.5-Severe Deterioration of an Amarillo Bent Cap.....	42
Figure 2.6-Single Column Directly Under a Construction Joint in Amarillo.....	43
Figure 2.7- Deterioration of Columns Due to Salt Laden Snow Piled against the Column.....	44
Figure 2.8-Horizontal Splitting of the Upper and Lower Reinforcement in a Typical Bent Cap.....	46
Figure 2.9-Face Splitting of a Bridge Column in Corpus Christi.....	47
Figure 3.1-Interaction diagram for the 18” Column Specimen.....	61
Figure 3.2-Section View, in Plan, with the Location of the P/T Bars.....	62
Figure 3.3-Section of the Column P/T Assembly.....	65
Figure 3.4- Installation of the Rubber Gasket at the Column-Foundation Interface.....	66
Figure 3.5-Schematic Diagram of Loading Plate and Foundation Detail.....	73
Figure 3.6-A Schematic Strut & Tie Model for the Foundation Under a Typical P/T Column.....	75
Figure 3.7-Plan View of Compression Struts after the 45 ° Rotation.....	80
Figure 3.8-Column Foundation Section.....	81
Figure 3.9-The Foundation Reinforcement Prior to Forming.....	82
Figure 3.10-The Foundation Layout.....	83
Figure 3.11-The Pipe Sleeves for the Service Load Post-Tensioning Bars Prior to Casting.....	84
Figure 3.12-The Completed Column Specimen Forms on Foundation No. 1.....	87
Figure 3.13-The Bottom of the Column Cage Illustrating the Duct.....	88
Figure 3.14-Casting Columns on Foundation No. 2.....	89
Figure 3.15-Stressing of Column P/T Bars.....	95
Figure 3.16-Service Load being Applied to a Column Specimen.....	99
Figure 3.17- Wiring Schematic of the Load Cell to the Voltmeter.....	100
Figure 3.18-The Column Irrigation System.....	103
Figure 3.19-Irrigation Termination Ends and Column Gridlines.....	104

Figure 3.20-Individual Column Designations	105
Figure 3.21-Long Term Column Exposure Tests Specimen Notation	106
Figure A.1-Half-Cell Potential for NJ-TC-S	120
Figure A.2- Half-Cell Potential for DJ-TC-S	121
Figure A.3- Half-Cell Potential for DJ-FA-S	122
Figure A.4- Half-Cell Potential for DJ-TC-N	123
Figure A.5- Half-Cell Potential for NJ-TC-N	124
Figure A.6- Half-Cell Potential for PT-TC-N-PD.....	125
Figure A.7- Half-Cell Potential for PT-TC-S-PD	126
Figure A.8- Half-Cell Potential for PT-FA-S-PD	127
Figure A.9- Half-Cell Potential for PT-TC-S-EB	128
Figure A.10- Half-Cell Potential for PT-TC-GB	129
Figure C.1-Foundation Reinforcement, Plan View.....	198
Figure C.2-Column Post-Tensioning Section	199
Figure C.3-Bar Details for Foundations.....	200
Figure C.4-Column P/T Bars in Section	201
Figure C.5-Foundation Section	202
Figure C.6-Column Loading Plate Details	203
Figure C.7-Column-Foundation Connection Detail, “No Joint”	204

Chapter 1

Introduction

1.1 General Bridge structures in this country and abroad are currently undergoing significant changes in design. The single most significant adaptation began in the early 1800's, when prestressing was used by cooperage shops to band metal hoops around wood slats to form barrels. Prestressing and post-tensioning have been an intricate part of structural design and construction since this adaptation. P.H. Jackson (1), in 1886, is generally credited as the first engineer to introduce internal stresses by tensioning steel reinforcement. In Jackson's design, he patented the use of prestressed steel rods in floor slabs. These early attempts offered very little actual prestress force because of significant losses due to creep and shrinkage. Prestressing remained relatively stagnant until 42 years later when E. Freyssinet of France developed a prestressing force using high tensile steel wire.

This prestressing force, stemming from Freyssinet's original work, began to take shape in two distinct forms, pretensioned and post-tensioned. Post-tensioned refers to reinforcement that is tensioned after the concrete is cast and pretensioned refers to reinforcement that is tensioned prior to casting. Post-tensioning is the process that was used by Freyssinet. Since Freyssinet's first post-tensioned applications, post-tensioning has been used to solve many of the world's most difficult engineering challenges. These challenges include foundation problems, large concrete cylinder structures, containment structures in the nuclear power industry, high rise construction, and tall slender towers and bridge construction. The United States has long been the leader in pretensioned girders for short and medium-span bridges and for precast building frames. The use of post-tensioning has grown more slowly in the United States. The most common forms of post-tensioning application in bridge construction are in bridges with medium to long-span range and in long spans. The more common types of post-tensioned bridges include cast-in-

place box girders, balanced cantilever segmental bridges, and cable stay bridges. Segmental bridges for moderate span length because of their efficient form, elegant appearance and new ingenious construction techniques, have become increasingly popular in this country. Today, more than ever before, post-tensioning is in widespread use in this country and in Europe.

1.2 Substructure Design and Construction

1.2.1 General Design Concepts for Reinforced Concrete. Reinforced concrete is the term applied to concrete containing non-prestressed reinforcing bars designed to resist any tension that may occur in the member. In Texas, virtually all bridges constructed today contain some reinforced concrete. The concrete is described by “Class” which identifies a concrete’s strength, cement content, water cement ratio, and coarse aggregate type. These particular classes of concrete can be found in “The Texas Department of Transportation Standard Specifications for Construction of Highways, Streets, and Bridges.”(9) Concrete used for reinforced concrete in Texas must meet the requirements of these specifications. Generally, the use of fly ash to replace some of the cement in the concrete is gaining acceptance. However, fly ash is still limited to 35% replacement by volume. Reinforcing steel design is based on “The American Association of State Highway and Transportation (AASHTO) Specifications” (10).

Reinforcing steel is generally Grade 60 except for spiral reinforcement. Spiral reinforcement can be either hot rolled or cold drawn steel. Design practice for substructures is well documented in AASHTO. However, some of the more general observations that are relevant to this thesis are:

- The Modulus of Elasticity for reinforcing steel is taken as 29,000 ksi.
- For flexural calculations linear strain variation is assumed.
- For Service Load Design, stress in the steel is the Modulus of Elasticity times the calculated strain.

- For Load Factor Design, stress in the steel is the Modulus of Elasticity times the calculated strain except that, where the strain exceeds 0.00207, the stress is at yield of 60 ksi.
- Spiral reinforcing used for ties in columns should be a No. 3 at a 6-inch pitch for 30-inch columns and smaller columns and No. 4 at 9-inch pitch for larger columns.
- Longitudinal reinforcing in columns should have an area of at least one- percent of the gross concrete area, regardless of the relationship between actual and required capacity.
- Splicing of bars should be avoided in an area where reinforcing from an intersecting member exists.
- Splicing cap bars over a column should be avoided.
- Compression splices in flexural members are not recommended.
- Splicing in regions of maximum stress is not recommended, but is permissible.

To retain close agreement with the Texas Department of Transportation's general practices, the column specimens cast for this thesis will comply with all of the Department's Specifications as well as these general guidelines. The TxDOT Specifications (9), as they pertain to durability, deal only with cover of the reinforcement and class of concrete.

Inherent in reinforced concrete is cracking. To some extent all reinforced concrete substructure components crack. The influence of cracks and in particular crack width has been a controversial subject for some time. The American Concrete Institute, ACI, in a committee report presents the two most common points of view. They are (8):

1.) Cracks reduce the service life of the structure by permitting a rapid means of access for moisture, chloride ions and oxygen to reach the reinforcement and accelerate the onset of corrosion.

2.) Cracks may accelerate the onset of corrosion. However, such corrosion will be localized to the region of the crack. This localized chloride propagation is thought to be less critical over time than the permeability of the concrete. Thus, this theory assumes that the difference between the rate of corrosion due to the localized cracking versus the actual permeability of the concrete matrix will be negligible.

The primary difference between reinforced concrete and post-tensioned concrete, from a durability standpoint, is post-tensioning's ability to control crack widths and significantly reduce cracking. This should be extremely helpful if the first of these theories is correct. It would be less helpful if the second theory is correct. Additional benefits include the reduction of reinforcement thereby reducing congestion and enhancing workability.

1.2.2 Post-tensioned Concrete. Traditionally the substructure components of a bridge were dominated by timber construction in the late 1800's, then by steel and later by reinforced concrete. Timber and steel diminished in the late 1960's in Texas due primarily to their susceptibility to corrosion and rotting. Early reinforced concrete construction also had substantial durability problems with a susceptibility to corrosion. Over the years improvements in concrete quality, greater cover and bar coatings were introduced in order to reduce this susceptibility. Because of improved corrosion resistance it is likely that prestressing will begin to dominate substructures just as reinforced concrete dominated substructure design in Texas from late 1950's to the 1990's. Since 1978 the National Bridge Inventory has and is currently appraising

all on-system bridges in the United States. The results are significant. The rating system has index numbers. The meaning for each index number is given in Table 1.

Table 1.1: Index Numbers for The National Bridge Inventory Rating System

Rating	Description
9	Conditions(s) superior to present criteria.
8	Condition(s) equal to present desirable criteria.
7	Condition(s) better than present minimum criteria.
6	Condition(s) equal to present minimum criteria.
5	Condition(s) somewhat better than minimum adequacy to tolerate being left in place.
4	Condition(s) meeting minimal tolerable limits to be left in place.
3	Basically intolerable condition(s) requiring high priority of repair or reconstruction.
2	Basically intolerable condition(s) requiring high priority to replace the structure.
1	Immediate repair or reconstruction necessary to put the structure back in service.
0	Immediate replacement of the structure necessary to put back in service.
N	Not Applicable

Of the 327,829 bridges recorded, 45,587 are reported as deficient (Marginal Condition). There are several factors and limits that substantiate this claim. They are:

- Only bridges constructed after 1950 were considered.
- Only structures spanning a length greater than 20 feet were considered.
- Only deficiencies as the result of condition rating of 4 or less for deck, superstructure and substructure or an appraisal rating of 2 or less for structural condition were considered.

A further breakdown of this data is given in Table 1.2.

Table 1.2: Breakdown of the Deficient Structures Nationally

	Inventory Units	Structurally Deficient Units	Percentage
Concrete			
Reinforced	91,886	6,027	6.6
Prestressed	88,304	3,212	3.6
Structural Steel	118,424	22,928	19.4
Timber	27,817	13,199	47.4
Other	1,309	214	16.3
Totals	327,829	45,587	13.9

Table 1.2 illustrates the superior performance of prestressed concrete. Prestressed concrete, in addition to its performance, has gained an increased share of the bridge structure market since 1950. The increase in this material's market share is due in large part to the materials economic benefits. The NBI data can also be used to make actuarial life expectancies. As expected, prestressed concrete has the highest actuarial projection based on a 95 percent confidence interval. This increase in longevity further solidifies prestressed concrete's place in future bridgework. Obviously, corrosion prevention in this area needs to be addressed to be prepared for this increase in usage (20).

Figure 1.1 illustrates the segmental post-tensioning procedure in which the reinforcement is tensioned after the concrete is cast.

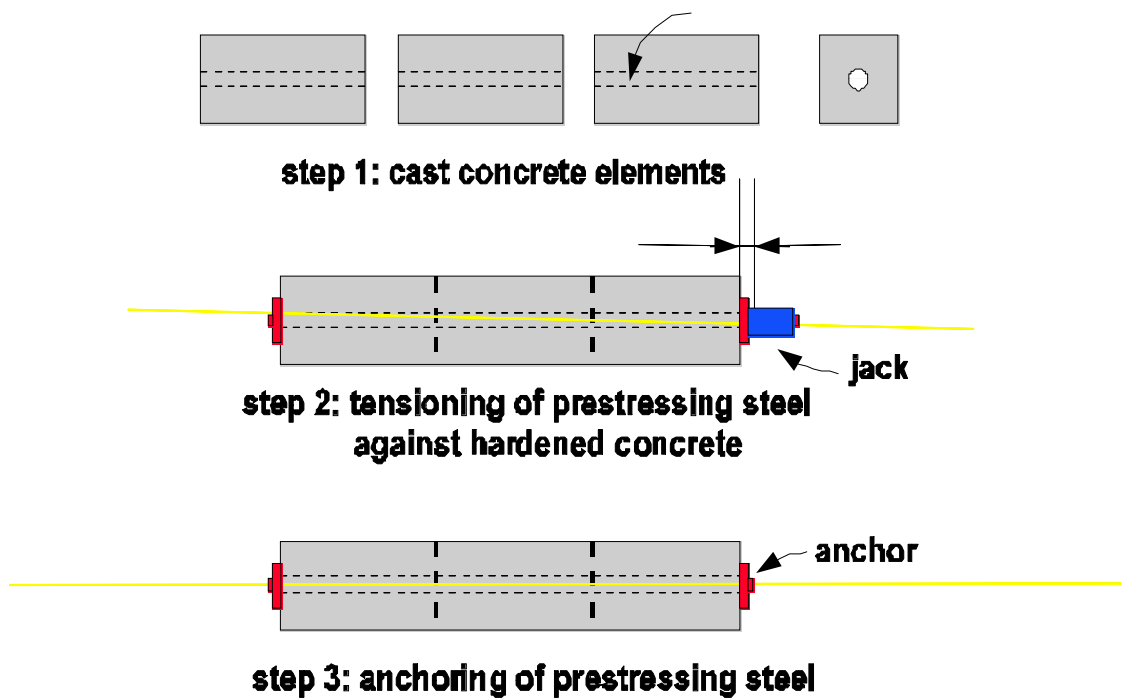


Figure 1.1: Post-tensioning Schematic

As shown in Figure 1.1, after the concrete is cast the segments are pulled together by tensioning the high strength steel against the hardened concrete using special jacks. Once the jacking operation is completed, the tendons are grouted for bonded construction or greased if the construction method is unbonded. In unbonded post-tensioning, the steel is only attached to the concrete member at the member's end anchorage. The use of either system is dependent upon the application. Both systems however, have corrosion prevention measures. The unbounded tendons are generally used in applications with low friction and small ducts where economical considerations outweigh the corrosion concerns. Even so, the strands are greased and special protection is provided at the end anchorage.

The bonded system uses grout injected into the duct. This system with its improved resistance against exposure to the elements and the additional structural benefits of being fully bonded is generally preferred in bridge construction.

In general, post-tensioning uses propriety systems. Several systems are available on the market today. The predominant systems are monostrand, multi-strand or single-bar tendons. The leading manufactures of these systems are Freyssinet K-Range, VSL and the Dywidag (DSI) system. The Freyssinet, VSL and DSI systems all employ multi-strand tendons. Each strand is gripped by a three-piece conical jaw, which sets in a tapered hole. The taper is such that the jaws are forced closed onto the strand during post-tensioning.

The Dywidag bar post-tensioning system employs high strength bars that have coarse continuously rolled threads. These threads allow for ease of coupling in any location and are positively anchored by means of an anchor plate and nut or a bell shaped anchor and nut. Because of their much larger diameter, bars usually have much greater corrosion resistance than strands. The vertical elements, the columns, used in this thesis are post-tensioned with the Dywidag single bar system.

The maximum jacking stress (temporary) may not exceed $0.80f_{pu}$ and the transfer stress (lockoff) may not exceed $0.70f_{pu}$. In addition to these requirements by the manufacturer, this system for these columns must also satisfy AASHTO and TxDOT requirements.

The critical TxDOT post-tensioning requirements for the vertical column elements used in this project are:

- For grouted tendons, end anchorages and tendon couplers shall develop a minimum of 95 percent of the required ultimate strength of the tendon with a minimum elongation of two (2) percent of the gage length when tested in the unbonded condition.
- Polyethylene ducts shall be sufficiently rigid to withstand placement of concrete, grouting, and construction loads without damage or excessive deformation, while remaining watertight and shall be in accordance with ASTM designation D3350.

- Plastic material used shall not react with concrete or enhance corrosion of prestressing steel and shall be free of water-soluble chloride.
- The inside diameter of the duct shall be at least 1/4 inch larger than the normal diameter of a single strand, bar, or wire tendon; for multiple strand or wire tendons, the inside cross-sectional area of the duct shall be at least two (2) times the net area of the prestressing steel.

In addition to the duct and elongation requirements there are several grout specifications that will be addressed in the scope of this research. They are:

- The ducts must be grouted within 48 hours after the completion of the tensioning operation.
- The temperature of the concrete must be maintained between 35 F and 90 F.
- Grout shall be pumped continuously under moderate pressure at one end until all entrapped air is forced out of the vented end downstream from the grout pump.
- Grout ports shall consist of 1/2" diameter pipe, with caps and valves.

The specifications listed above are the predominant TxDOT guidelines for post-tensioning. In general, there are no provisions for the protection of the end anchorage or any additional durability provisions. The grout does require an expansive admixture to prevent voids in the duct system and to insure a completely grouted and bonded tendon.

As mentioned previously, reinforced concrete inherently cracks. Post-tensioning can minimize the cracking. Post-tensioning should reduce not only the adverse effects of cracking in flexure but shrinkage cracks as well. Thus, it should substantially enhance the column's overall resistance to permeability.

Post-tensioning's biggest advantage over reinforced concrete is its ability to control the crack width.

1.3 Corrosion of Reinforcing Steel in Concrete. Corrosion is defined as the destruction or deterioration of a material because of reaction with its environment (7). Corrosion can be considered as extractive metallurgy in reverse. Iron ores contain a significant amount of iron oxide. Extractive metallurgy is the process of extracting a

metal from the ore and refining the metal for use. The reverse process is where corrosion returns the metal to iron oxide or 'rust', the common name reserved for iron oxide.

1.3.1 Corrosion Principles This change from metal to iron oxide is a thermodynamic change that is best described as a change in free energy. Furthermore, this free energy change is an electrochemical reaction. This free-energy change accompanying an electrochemical reaction can be calculated by the equation:

$$G = -nFE \quad (1-1)$$

1)

where G is the change in free energy, *n* is the number of electrons involved, F is the Farady constant and E is the cell potential. To further illustrate the concept of cell potential consider an example of a replacement reaction with copper and zinc. The replacement reaction at equilibrium is given as:



The equal sign represents an equilibrium condition in the equation above. To keep the bookkeeping simple, the concentrations of metal ions are at unit activity and the solutions each contain approximately 1 gram-atomic weight of metal per liter. This configuration can be illustrated as shown schematically in Figure 1.2.

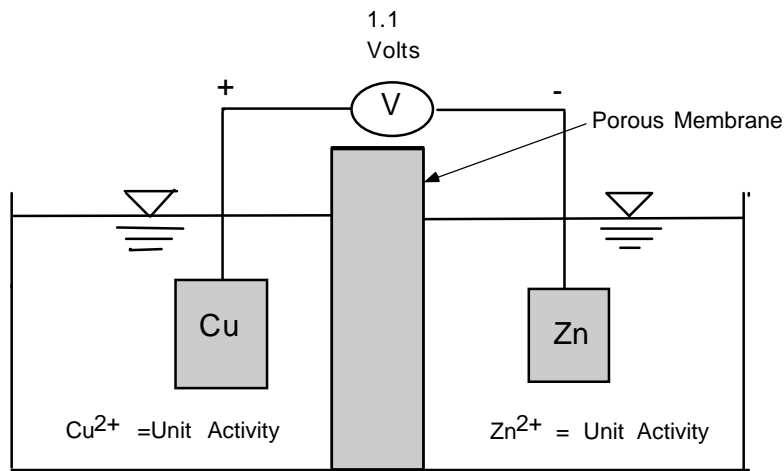


Figure 1.2- Copper and Zinc with their Ions at Equilibrium (6)

Since both electrodes are at equilibrium and the system is maintained at unit activity the rates of metal dissolution and deposition must be the same. Figure 1.2 illustrates this effect. Note that for each copper atom that is oxidized to cupric ions, there are cupric ions that are reduced to copper. These conditions of unity and equilibrium mean that the rates of these reactions are equal. Therefore, the rate of metal dissolution, r_1 , is equal to the rate of metal deposition, r_2 . Figure 1.3 illustrates this system and the deposition and dissolution of metal.

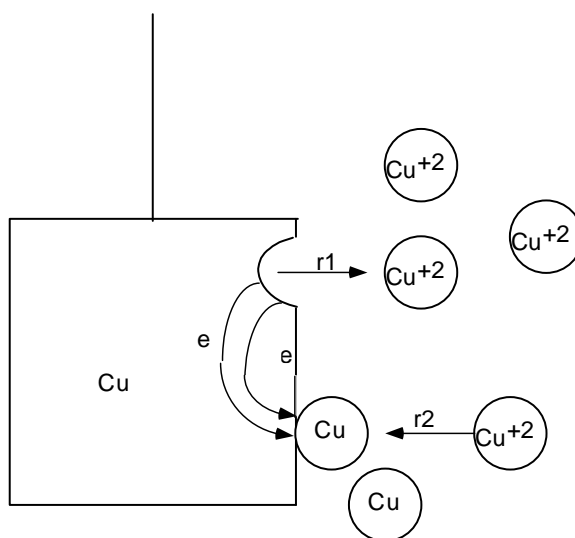


Figure 1.3- Reversible Copper Electrode (6)

This system at equilibrium with unit activity is termed a standard half-cell reaction. All electrochemical reactions can be determined in this manner. To reference the potential difference in the standard half-cells, the hydrogen ion ($2\text{H}^+ + 2\text{e} = \text{H}_2$) reaction is used and universally accepted as the zero reference point. The cells potential difference is the free energy of the system. In other words the free energy is the electrical difference or electromotive force (emf) of the system. In the example shown in Figure 1.3 the dissolution of copper to cupric ions ($\text{Cu} = \text{Cu}^{2+} +$

2e) has a potential of + 0.337 at a standard temperature of 25° C versus the normal hydrogen electrode potential. Table 1.3 presents the standard half-cell potential for several pertinent reactions.

Table 1.3- Standard EMF Series* (6)

Reaction	Standard Potential (volts vs. SHE ^a)
$O_2 + 4H + 4e = 2H_2O$	+1.229
$Fe^{3+} + e = Fe^{2+}$	+0.771
$O_2 + 2H_2O + 4e = 4OH$	+0.401
$Cu = Cu^{2+} + 2e$	+0.337
$2H^+ + 2e = H_2$	0.000
$Fe = Fe^{2+} + 2e$	-0.440
$Cr = Cr^{3+} + 3e$	-0.744
$Zn = Zn^{2+} + 2e$	-0.763
$Al = Al^{3+} + 3e$	-1.662

^a Standard hydrogen electrode

1.3.2 Half -Cell Potential. The preceding figure, Figure 1.3, demonstrates anodic and cathodic reactions. Anodic reactions, r_1 , are reactions where electrons are given off and the metal is dissolved. Cathodic reactions, such as r_2 , in Figure 1.3, are reactions that consume the electrons given off at the anode. This gaining and simultaneous loss of electrons is described as *redox equations*, or oxidation-reduction equations. The gaining of electrons at the cathode is termed a reduction reaction and the loss of electrons or oxidation occurs simultaneously at the anode. The solution or electrolyte, is the transport mechanism for these reactions. As the positively charged ions released from the anodic surface combine with the negatively charged ions from the cathodic surface, current begins to flow and the onset of corrosion begins.

In the corrosion of reinforcing steel, the anodic process, or metal dissolution, is given by:



The electrolyte for reinforcing corrosion is the surrounding concrete and the presence of oxygen and water that is contained within the concrete. At the cathode, an entirely different reaction occurs. The cathodic reaction is driven by the reduction of water and oxygen contained within the solution. The corresponding half-cell equation is given by:



This equation indicates that the driving force behind reinforcing corrosion is the amount of oxygen and water available to complete the reaction. As the cathode consumes electrons the cathodic half-cell releases hydroxyl ions (OH⁻) into the solution. Combining the half-cell equations from both the anodic and cathodic reactions yields:



The product of this reaction is unstable in atmospheric conditions and stabilizes itself with more oxygen to form the familiar reddish-brown colored substance called rust (12). This ‘rust’ equation is given as:



This type of corrosion in reinforced concrete can occur in one of two ways. The corrosion can occur as a ‘microcell’ or a ‘macrocell’. Corrosion in either system is the same electrochemical process. However, microcell corrosion refers to both the cathode and the anode belonging to the same piece of reinforcement. Microcell

corrosion can be very severe due to an area effect. Generally microcell corrosion is due to a small break in the passive layer. This break then leads to a relatively small anode and the rest of the reinforcing bar acts as a cathode. The corrosion due to an area effect (because of the larger area of the cathode) may be 100 to 1000 times greater than the corrosion of two equal areas.

Conversely, macrocell corrosion is established when a galvanic cell is set up within a reinforced member. When considering a substructural component such as a bridge column, a galvanic cell can be set up between two vertical reinforcing bars while the spiral acts as a salt bridge.

The accepted practice to determine if reinforcing steel in reinforced concrete is corroding is a half-cell survey. This test should be conducted in accordance with ASTM C 876 “Standard Test Method for Half-Cell Potentials of Uncoated Reinforced Steel in Reinforced Concrete.” (8)

The procedure for this test consists of placing a reference electrode at desired intervals upon the surface of the concrete. These intervals should be at regular distances and mapped to obtain several readings. A second lead wire is connected to the reinforcement that is suspect to corrosion activity. The reference electrode wire and the second wire are then connected to a volt meter and the voltage is read directly. By convention the sign of this voltage is negative. This driving force is an indication of the concentration of Fe^{2+} ions in the concrete surrounding the reinforcement. This indirect reading of ferrous ion concentration can determine the probability of corrosion. ASTM categorizes the probability of corrosion into three groups according to potential from the voltmeter, they are:

- More positive than -0.20 V. CSE, there is less than a 10 percent probability that corrosion is occurring;
- Between -0.20 and -0.35 V. CSE, there is an uncertain probability of corrosion occurring;

- More negative than -0.35 V. CSE, there is a 90 percent probability of corrosion occurring.

The ASTM C 876 is just one method to determine the onset of corrosion. The concentration of ferrous ions within the concrete can vary as the areas of steel become more or less anodic. This is especially true with microcell corrosion. To determine the extent of corrosion activity in the reinforced specimens contained within the scope of this research, the half-cell potential will be one of several tests. The results of the half-cell tests by themselves will not be taken as a direct indication of corrosion activity. This test will be coupled with several tests including a linear polarization corrosion test to further identify areas of corrosion and their propagation.

1.3.3 Rate-of -Corrosion. Engineers use kinetics to determine the rate of corrosion. As in the previous half-cell discussion, equilibrium states that the reduction rate must equal the rate of oxidation. When corrosion is present, the half-cells become ‘short circuited’. Therefore, the potentials of these electrodes, the anode and the cathode, will no longer be at their equilibrium potential. This deviation from the equilibrium potential is called polarization. This is not to suggest that the system changes. In fact, the free energy change for the anode and the cathode are equal. The magnitude of the polarization is measured in terms of ‘overvoltage’. Overvoltage is measured in millivolts or volts with respect to equilibrium potential.

Even at the equilibrium condition there is a rate at which the anode oxidizes and the cathode reduces. This finite rate is defined as the exchange current density. The exchange current density is derived from Faradays Law and can be expressed as:

$$r_{\text{oxidation}} = r_{\text{reduction}} = i_0/n F \quad (1-7)$$

where $r_{\text{oxidation}}$ and $r_{\text{reduction}}$ are the equilibrium oxidation and reduction rates, i_0 is the exchange current density, n is number of electrons transferred and F is

Faraday's constant. (6) This shift in potential or overvoltage can be defined by the Tafel Equation (8).

The equation can be expressed as:

$$\eta_c = \beta_c \log (i_c/i_o) \quad \text{or} \quad \eta_a = \beta_a \log (i_a/i_a) \quad (1-8)$$

where c is the Cathodic polarization or overpotential and consequently a is the anodic polarization. In addition, note that the respective subscripts 'a' and 'c' also denote the exchange current density. These concepts of kinetic equations define the basis of modern electrode-kinetics theory or mixed potential theory. The point at which the total rate of oxidation equals the total rate of reduction is the mixed or corrosion potential of the system. The corresponding point, as illustrated in Figure 1.3, is the exchange current density. This point is where the half-cell electrode potentials are equal. This corrosion rate, i_{CORR} , is inversely proportional to the polarization resistance.

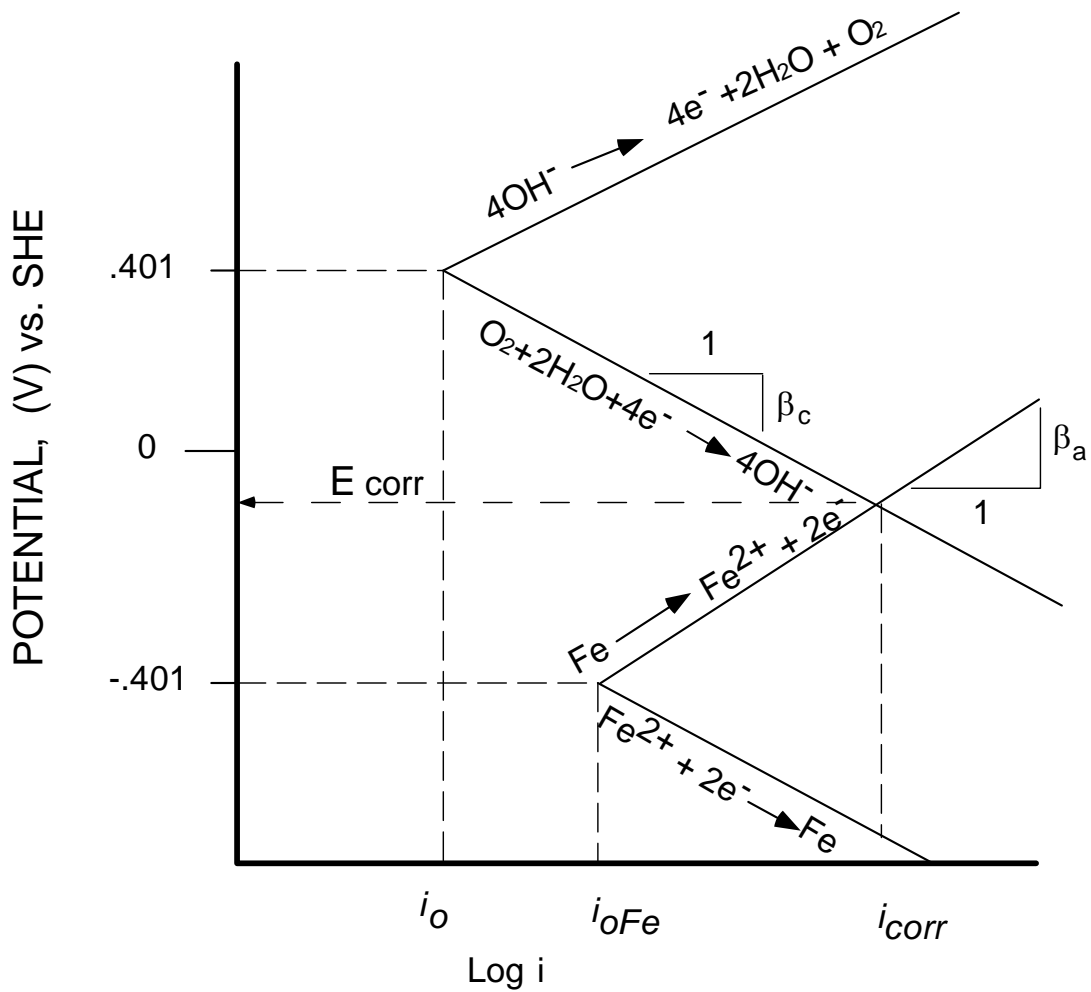


Figure 1.4- Polarization Diagram for Reinforced Concrete

The most common test method corresponding to this theory is called the linear polarization test. This test uses a plot of applied exchange current density (i_{app}) versus corrosion potential (E). The intercept of this axis is an overvoltage reference

point and thus the slope of this linear polarization curve relates to the kinetic parameters of the system as follows:

$$E/i_{app} = \frac{\beta_a \beta_c}{2.3(i_{corr})(\beta_a + \beta_c)^{(3)}} \quad (1-9)$$

The term E/i_{app} is given in ohms (volts/amperes). As Equation (1-9) shows, once the values are known the corrosion rate, i_{corr} can be determined. In addition, i_{corr} is relatively insensitive to beta values. Therefore, it is possible to formulate a reasonable approximation of this equation. To give the corrosion rate a physical meaning an exchange current density of $1\mu\text{A}/\text{cm}^2$ roughly corresponds to a corrosion rate of 0.5 mills penetration per year (mpy). For iron, the exchange current density is approximately equal to 0.46 mpy (12).

The corrosion rates established from the linear polarization technique need to be taken at several uniform intervals to establish the polarization curve and to yield accurate data. As this technique, linear polarization, pertains to reinforced concrete some common thresholds relating to corrosion of the reinforcing have been established by Mars Fontana (6). They are as follows:

- i_{corr} less than 0.20 mA per square foot- no corrosion damage expected;
- i_{corr} between 0.20 and 1.0 mA per sq. ft.- corrosion damage possible in the range of 10 to 15 years;
- i_{corr} between 1.0 and 10 mA per sq. ft. - corrosion damage expected in 2 to 10 years;
- i_{corr} in excess of 10mA per sq. ft. - corrosion damage expected in 2 years or less.

This test coupled with the standard half-cell test addressed in section 1.3.2 has the potential to lead to excellent results. All of the specimens from Project 1405 have been prewired to facilitate both of these tests.

1.4 Research Objectives. The primary goals of the research contained herein are twofold. The first goal, is to define the Texas Bridge substructure problems as these problems relate to durability. This was accomplished by employing the National Bridge Inventory and Appraisal System (BRINSAP) to determine the percentage of substructures with significant corrosion. BRINSAP was used to divide Texas into geographic regions with similar corrosion concerns as these concerns related to substructures. The second goal is to develop an experiment which would use accelerated long-term exposure tests to replicate the findings of the BRINSAP study. Early on in the project, significant durability problems were uncovered in the initial BRINSAP survey (see Appendix A for BRINSAP data). As many as 2000 Texas bridges are experiencing substructure durability attack.

BRINSAP was also used to investigate trends in the types of superstructure and substructure which are experiencing durability attacks as well as a general replacement value for these structures, by the owner, the State of Texas. To determine an approximate estimate as to the financial extent of substructure durability attacks BRINSAP data can be used to determine:

- The average number of spans
- The average daily traffic
- Type of substructure design
- Extent of the durability attack
- Average longevity of the structures for a specific area.

Specific indications were determined by the author from the BRINSAP study. First, because of the large number of bridge substructures in Texas experiencing some type of corrosive attack, Texas did in fact have a substructure durability problem. Second, this durability problem is more pronounced in two distinct regions, the coastal region and a region of Northwest Texas defined by the Federal Highway Administrations (FHWA) de-icing line (see durability map in Figure 2.1). Additional questions regarding the variability were:

- Is the mechanism of the attack specific to a specific substructure component?
- Is the attack independent of the geographic region?
- Is the corrosion mechanism the same throughout the state?
- Is the corrosion mechanism the same throughout the region?

In Texas bridge columns, in both the coastal region and the northwest region, the corrosive attack was very prevalent and the attack was very similar in nature. During field investigations of several bridges in both Corpus Christi and Amarillo, Texas, it was determined that the corrosive attack occurred at approximately the same location on the columns relative to the water or snow line on the bridge column. Therefore, the research indicates that specific corrosive attacks to the substructure components and used to design an experiment to simulate steel corrosion and determine the effects of variables using scaled experiments, were not limited to geographic considerations thus suggesting an answer to the questions above.

To evaluate the corrosion mechanisms that are prevalent in Texas Bridge columns, an experiment would use conventional reinforcing and Class C concrete as a base case. A method of simulating an aggressive attack would be developed. In order to compare the methods of protecting columns, various methods using post-tensioning and other column design would be studied. This would allow one to evaluate the corrosion mechanism against current and future column designs.

Furthermore, these specimens should be subjected to all of the loading conditions which would be imposed on conventional columns in order to simulate cracking. This would include both applied loads and moments.

1.5 Scope. In the following chapters a study of the development of a test procedure and the evaluation of tests to determine the effects of using post-tensioning versus conventional reinforcement for bridge columns is presented as a means of improving substructure corrosion resistance. Chapter 2 covers the BRINSAP Inspection program in Texas, the results of the project substructure survey, the survey data and field condition survey. In addition, Chapter 2 covers the results and recommendations that the BRINSAP survey suggests. The test setup to study the corrosion aspects in the scale columns is given in Chapter 3. Also, the test setup, design and development, materials, and variables, specimen preparation, loading and water ponding, as well as the test procedure are given in Chapter 3.

The results for the active specimens and the recommendations for the active and inactive specimens are presented in Chapter 4. In addition, there is some discussion as to future study. Finally, in Chapter 5, the thesis is summarized and conclusions and recommendations are presented.

Chapter 2

BRINSAP DATA

2.0 Introduction. The Bridge Inspection and Appraisal Program (BRINSAP) in Texas is the current method by which TxDOT routinely inspects, manages and maintains each of the state's 'On-System and 'Off-System' bridges. As part of this ongoing inspection a complete database of all of the state's 33,640 On-System bridges are kept on computer files. This data can be reduced to pertinent aspects of the structure, such as substructures, and further reduced to determine the material composition of the substructure. Through this database, initial determinations regarding the condition of Texas bridges concrete substructures were made.

In this chapter the number of distressed substructure conditions in Texas will be presented. These structures will be categorized by geographical areas in which the primary factor is corrosive attack. In addition, the factors, which contribute to a high replacement value, will be presented. These bridges, which represent approximately 8% of the Texas 'On-System' bridges, have a substructure rating of 5 or below. The fact that a bridge in this category has a rating of 5 or below does not automatically mean that the substructure is suffering from corrosive attack. BRINSAP does not currently distinguish between types of damage.

2.1 The Appraisal System. The primary evidence for corrosive attack in Texas Bridge substructure components can be found in BRINSAP data. In 1978, the Federal Governments "Code of Federal Regulations, 23 CFR 650 C" required that "each highway department shall include a bridge inspection organization capable of performing inspections, preparing reports, and determining ratings in accordance with the provisions of the American Association of State Highway and Transportation Officials (AASHTO) Manual and Bridge Standards." Of primary importance to this thesis are the BRINSAP's program objectives of:

- Maintaining an up-to-date inventory that indicates condition of all bridges on public roadways.
- Determining the extent of minor deterioration requiring routine maintenance and repair work as the basis for planning bridge maintenance programs.
- Determining the extent of major deterioration requiring rehabilitation or replacement as the basis for planning bridge replacement and rehabilitation programs.

These program objectives and the database associated with these objectives is the cornerstone for assessing the current substructure performance in each of TxDOT's 25 districts.

The system that BRINSAP uses for appraising each bridge substructure is given in Table 2.1. The individual deficiencies in the various features are evaluated as to how they affect the safety and serviceability of the bridge as a whole. The intent of the appraisal rating is to compare the existing bridge to a newly built one that would meet the current standards for the particular highway system of which the bridge is a part.

Table 2.1: The Rating Guide for BRINSAP Appraisal (13)

Rating	Description
9	Excellent condition
8	Very good condition-no problems noted
7	Good condition-some minor problems
6	Satisfactory condition-minor deterioration of structural elements (limited)
5	Fair condition-minor deterioration of structural elements (extensive)
4	Poor condition-deterioration significantly affects structural capacity
3	Serious condition-deterioration seriously affects structural capacity
2	Critical condition-bridge should be closed until repair
1	Failing condition-bridge closed but repairable
0	Failed condition-bridge closed and beyond repair
N	Not applicable

A rating of 5 is used to determine bridges which would be in need of replacement. As a subset of bridges the author categorized those bridges which have a rating of 5 or below where the prevailing factor in the damage is suspected to be corrosion. There is not a TxDOT requirement that the deterioration be corrosion. The BRINSAP report does not distinguish between deterioration and durability. Once corrosion is extensive, as the rating of 5 would suggest for a durability attack, the structural members become irreparable and should be replaced to arrest the corrosion. The appraisal rating of 5 was used as a baseline measure to establish the number of substructures in Texas with significant deterioration based on examination of a number of bridges so classified. This data was acquired through the BRINSAP database. The sample chosen is all of the On-System bridges in Texas. ‘On System’ is defined as any bridge on the State and Federal Highway System. State and/or Federal Systems include the following:

- Interstate Highways

- US Highways
- State Highways
- State Loops or Spurs
- Farm or Ranch to Market Roads
- Park Roads
- Recreation roads
- Metropolitan Highways (Federal-Aid Urban Systems)

2.2 Initial BRINSAP Findings. Texas is an extremely large state with significant changes in geography, topography and more significantly, climate. To assess Texas bridge substructures with the aid of the BRINSAP data, a ‘sample’ of on-system bridges with a substructure rating of 5 was selected from all of the on-system bridges in Texas. This sample represents 10% of the On-System bridges in Texas. This sample was further subdivided into the State of Texas’s respective counties, although not all of the states’ counties have On-System bridges with a substructure rating of 5 or below. The primary interest in the sample is the age of the structure. This statistic is reflective of the durability impact on the longevity of the structure. The age of the structure was also used to map the areas of low longevity. These areas were grouped in the study by district. The significance of the district areas with more or less longevity will be addressed further in the Field Study portion of this report. Table 2.2, lists other significant variables from this sample. The values shown are indicative of the state On-System Bridges with a substructure rating of 5 or below for the entire state.

Table 2.2: Pertinent Variables in On-System Bridges with a Substructure Rating of 5 or

Below

Description	Statewide
Mean Age	42 years old
Median Age	41 years old
Mean ADT (average daily traffic)	11,000
Median ADT	3,100
Mean Number of Spans	8.7
% of Bridges where Substructure Controls Longevity	70%

The most revealing statistic from Table 2.2 above is the percentage of bridges where the longevity is controlled by the substructure. The fact that 70% of the bridges are deficient because of substructure problems shows the key importance of substructure durability. If the substructure deteriorates to this replacement rating of 5 the entire structure must be replaced. The condition of the entire superstructure is put at risk because of a substructure deteriorating underneath it. In terms of replacement value the cost of infrastructure has now significantly increased. In rehabilitation work, several reinforced concrete decks have been replaced with the rest of the original structure intact. In fact, the bridge is generally widened at this point to accommodate an increase in traffic flow. However, a deteriorated substructure leaves the bridge designer no options except for complete replacement. As one would suspect the actual replacement versus rehabilitation cost for the State of Texas is very difficult to quantify and beyond the scope of this research. However, the fact remains that substructure deterioration in Texas among the structures in this sample is prevalent and the rehabilitation cost is very significant.

The state picture of the effects of the below standard substructure rating is illustrated in Figure 2.1. The map in Figure 2.1 depicts the districts with a low average or mean age of the structure. Significant among the districts is the very low median age of the bridges in the Texas Panhandle. Lubbock District has a mean age of 27.7 years and the Amarillo District is 30.6 years old. Currently, TxDOT is designing bridges for

an expected service life of 75 years (21).

The FHWA de-icing line is significant from the standpoint of dividing the geographic regions. There are 10 districts with bridges above the deicing line. Of those ten districts, eight have a mean age of less than 37.5 years or half of the required design service life from the sample of bridges with a deficient substructure rating.

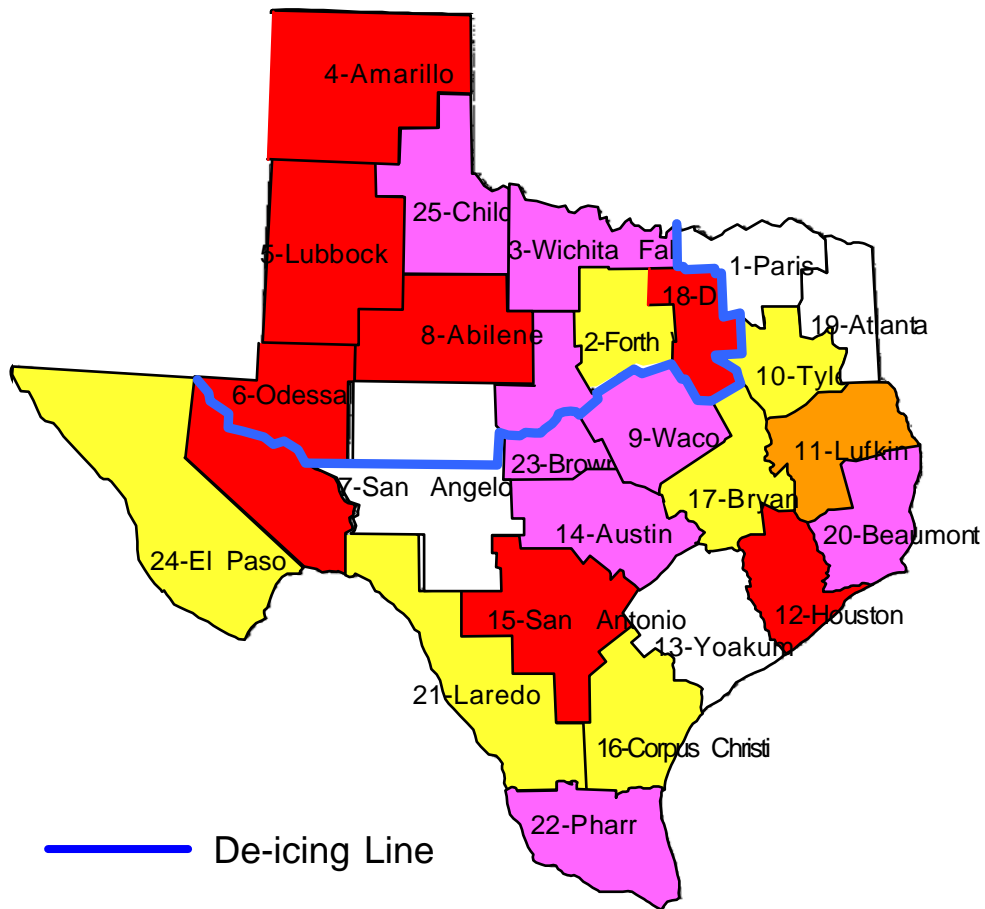


Figure 2.1: The State of Texas, by District Depicting Mean Age of Deficient Bridge Structures

The map of Figure 2.1 illustrates distinct regions and shows clear trends. The San Angelo district may be the exception as far as mean age. The ten districts, with a mean age from 25 to 37.5 years, are very close in the statistical categories extracted from the BRINSAP database. The evidence that the map does show, is a low median age at or above the deicing line and a low age near the coastal area. The sample size for the urban districts are large enough to be a representative sample. Houston, for instance, has 85 bridges with a substructure rating of 5 or below. The mean age of those 85 bridges is 30 years and this is considered an accurate number. Concern arises in some of the rural districts whose sample sizes are much lower. Lubbock is an example of a low sample size with a sample of 28 bridges representing the district.

A second problem arises in the actual data. The BRINSAP data does not distinguish between a durability problem versus some other type of substructure defect. An example of this effect could be a foundation problem. The bridge could experience settling problems where the damage is extensive and throughout. This type of structural defect was found to be quite rare but possible. A telephone survey of all 25 districts was conducted and the BRINSAP coordinators contacted. In general, these coordinators agreed that the possibility of a 5 rating with regard to substructures was in most cases a durability attack.

To further cloud the data, in the initial run from BRINSAP no provisions were made to include only concrete substructures in the sample. This error could include bridges with a timber or steel substructure. This problem was corrected by excluding steel and timber substructures to insure only concrete substructures in the sample of bridges. Steel substructures which have deteriorated to the condition rating of 5 will have to be replaced. Therefore, the initial BRINSAP data runs still have some significance as this data suggests a corrosive environment and an appropriate substructure design should be considered when TxDOT replaces these structures.

2.3 The Geographic Regions. In The State of Texas, because of its vast geographic size,

the corrosive environments are distinctive from region to region. To facilitate the effectiveness of this report and ongoing research the state was divided into 4 regions, each with a similar corrosive environment. The previous section illustrates this similarity in West Texas. The mean age figure from the sample of distressed substructures depicts several districts above the de-icing line with bridge longevity of approximately half of the design service life. The enhanced corrosion is in all likelihood due in large part to the chlorides introduced from the de-icing salts. Because of this common link, the de-icing line is used to define the geographic region, West Texas. To the east of the West Texas region is an area of Texas that includes the districts Paris, Atlanta, Lufkin and Tyler. These districts comprise the region named the Northeast Region. This particular region shares the sulfate corrosion phenomenon. The Central Texas Region is comprised of Bryan, Waco, Austin, San Antonio and El Paso. This region is named because these districts form a central band through Texas.

The Central region has a low probability of corrosion and Figure 2.1 bears this fact out. The exception is the San Antonio District where the mean age is in the 25-35 year range. These districts results are discounted due to the data's small population. The actual number of deficient substructures in San Antonio is 25 bridges or 1% of the total number of On-System Bridges. The Coastal Region, named because all of the districts have a gulf coast line, is the fourth region. The regions districts are Beaumont, Houston, Yoakum, Corpus Christi and Pharr. Similar to the West Region, this region along the gulf front suffers from severe chloride attack. Table 2.3 summarizes the respective districts in the associated regions.

Table 2.3: Durability Regions and Their Respective Districts

Region	District	Region	District
West		Northeast	

	Odessa		Paris
	Lubbock		Atlanta
	Amarillo		Tyler
	Childress		Lufkin
	Abilene	Central	
	Wichita Falls		Bryan
	Fort Worth		Waco
	Dallas		Austin
Coastal			San Antonio
	Beaumont		San Angelo
	Houston		El Paso
	Yoakum		Brownwood
	Corpus Christi		Laredo
	Pharr		

One of the goals of this research project in defining the Texas Bridge durability problem was to establish trends. The BRINSAP data suggests a pattern of corrosion among several districts and this thesis groups those districts together. The number of On-System bridges in Texas with a substructure rating of 5 or less is significant. TxDOT currently has 1,775 on-system bridges with a concrete substructure having a rating of 5 or less. The total number of on-system bridges in the state of Texas is 33,640 bridges. Thus, the sample of deteriorated concrete substructures represents 5.3 % of all the on-system bridges in Texas.

In Section 2.2 there was some concern expressed as to the relative sample size on a per district basis. Table 2.4 gives a complete numerical breakdown for the on-system structures in Texas.

This table illustrates the relative percentages of bridges with a deteriorated concrete substructure. The mean is 5.3% and the median value is 4%. These numbers

are significant. Even the central Texas region districts have an average sample size of 28 deficient bridges per district. Brownwood and Laredo have a sample size below 25 bridges.

2.3.1 Replacement Cost. The replacement cost for bridges with substantial substructure deterioration is very significant. Assume an estimate of \$ 81,000.00 per span replacement cost (14). This cost is based on an average 2-lane bridge with an average span length of 80 feet. To replace the structures in Corpus Christi where the sample size of deteriorated bridges is 2%, and 69% of the bridges are controlled by substructure deterioration, is significant. The equation for the number of spans would be:

$$\begin{aligned} &\text{Number of bridges to replace because of substructure deterioration} \\ &= 1208 \times 0.02 \times 0.69 \\ &= 17 \text{ bridges} \end{aligned}$$

The actual cost would be:

$$17 \times 11(\text{number of spans}) \times \$ 81,000^{(14)}/\text{span} = \$ 15,147,000$$

This cost is based on replacing the bridges with a deteriorated substructure where the substructure is controlling the longevity of the bridge. In fact, the actual number of bridges to replace is the sample size of 24 bridges and this cost is approximately 21 million dollars. Furthermore the structures have an average life of 38.4 years, which means the structure will have to be replaced 1.9 times in a 75-year design service life. Figure 2.2, is a state map that illustrates the average number of spans for the structures with a substructure rating of 5 or below.

The Texas coast, because of the large number of saltwater bays and the inter-coastal waterway has several bridges with a significant number of spans. This high number of spans which adversely affects the replacement cost illustrates the severity of the substructure durability problem in Texas.

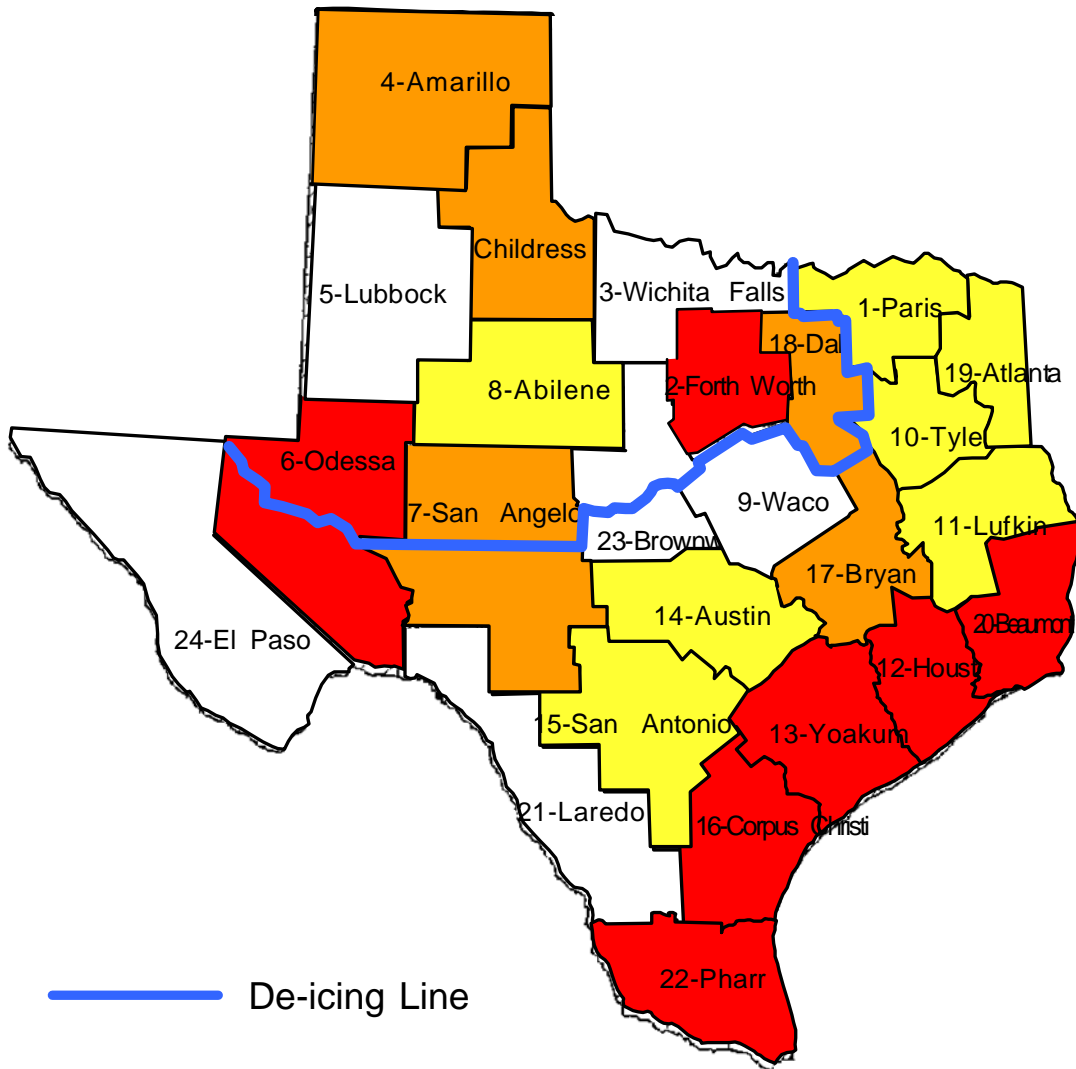
To further explain the magnitude of the problem, consider the value of a highway by the number of vehicles that a particular highway or structure serves per day. This daily average of vehicles is referred to as ‘average daily traffic’ or ADT. Significant amounts of traffic add additional dollar amount to the replacement cost of a structure. Shown in Table 2.4, is the ADT of the State of Texas for this particular sample, the structures with a substructure rating of 5 or below.

Table 2.4: A Summary of BRINSAP Data

District	On-System Bridges	Deficient Substruct . (%)	Age (Average)	AADT (Average)	Average No. Spans	Substruct. Controls (%)
1 Paris	1317	17%	41	2,045	7	63%

|

2	Fort Worth	2088	7 %	39	17,693	7	64%
3	Wichita Falls	1034	8%	37	3,496	6	53%
4	Amarillo	724	9%	31	12,390	9	65%
5	Lubbock	439	6%	28	4,574	4	82%
6	Odessa	1039	2%	34	5,133	12	75%
7	San Angelo	1188	1%	45	1,626	10	80%
8	Abilene	1371	4%	35	3,672	7	57%
9	Waco	1608	3%	36	8,409	6	70%
10	Tyler	1152	4%	40	3,248	8	87%
11	Lufkin	779	14%	36	2,757	8	83%
12	Houston	2861	3%	31	32,773	11	74%
13	Yoakum	1630	3%	41	2,334	14	91%
14	Austin	1592	3%	37	6,437	8	63%
15	San Antonio	2542	1%	30	18,132	8	96%
16	Corpus	1208	2%	38	2,222	11	69%
17	Bryan	1115	4%	39	3,472	10	82%
18	Dallas	3821	9%	34	24,406	10	73%
19	Atlanta	1087	7%	46	1,758	7	71%
20	Beaumont	1086	8%	37	14,671	11	74%
21	Laredo	782	1%	39	2,310	4	80%
22	Pharr	583	4%	36	5,834	11	96%
23	Brownwood	908	0.4%	35	1,193	5	100%
24	El Paso	981	3	38	7,756	6	84%
25	Childress	705	13%	37	742	9	37%



Number of Spans

- 11 - 14
- 9 - 10
- 7 - 8
- 4 - 6

Figure 2.2: Average Number of Spans/Bridge

Figure 2.3 indicates the cost and complexity of bridge replacement along the Texas coast as this cost relates to traffic concerns. In each of the coastal districts the average ADT exceeds 2000 vehicles per day. In three of the five coastal districts the ADT exceeds 4000 vehicles per day.

Houston has the most difficult conditions for bridge replacement. The Houston district has three very significant categories. They are:

- Low mean age of structures (30.5 yrs.),
- High average number of spans / bridge (11),
- High average ADT count (32,773).

The replacement cost for these deteriorated substructure structures, using a 10% increase per 10,000 ADT to reflect traffic control costs and effects, and the assumptions given earlier is:

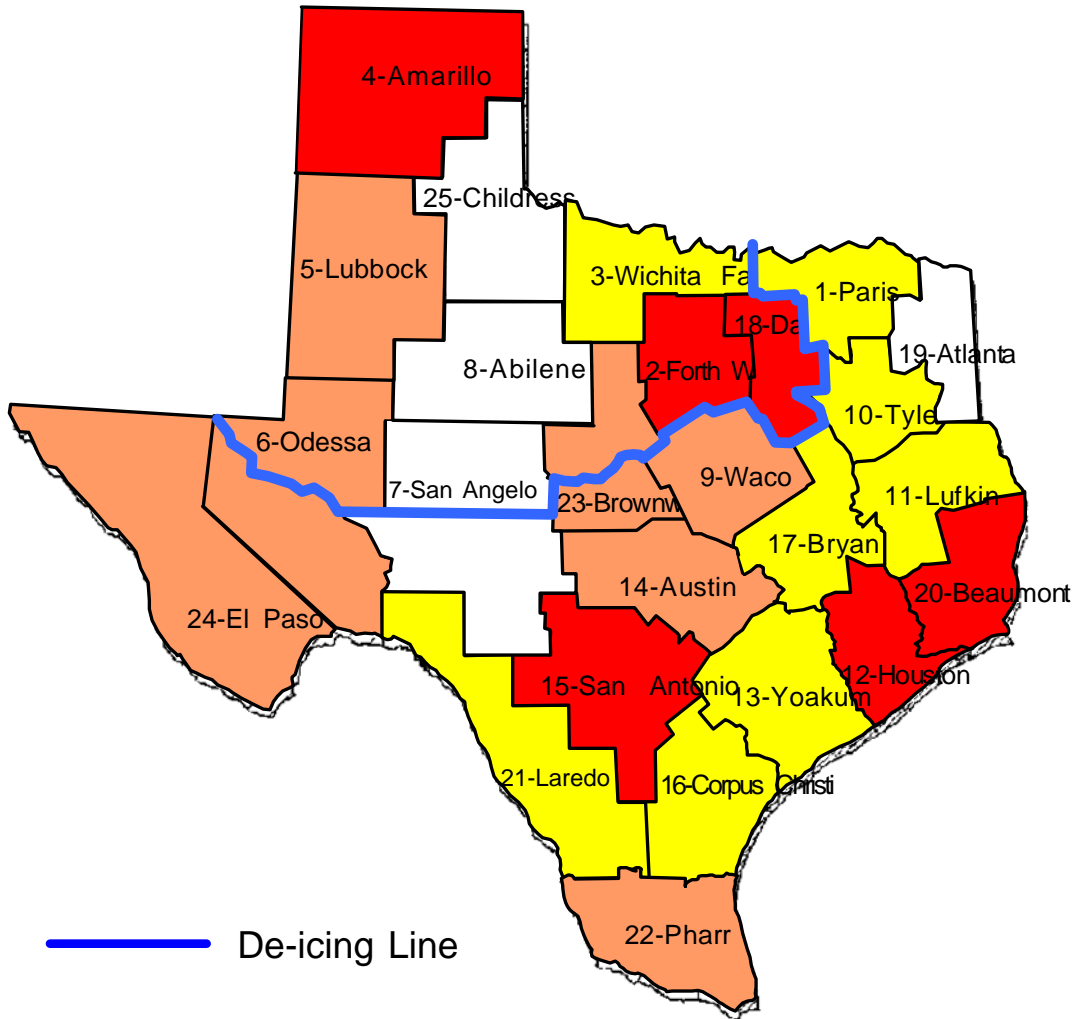
$$\begin{aligned} &= 1.3 \times 11 \text{ spans} \times 85 \text{ bridges} \times \$81,000/\text{span} \\ &= \$98,455,500 \end{aligned}$$

Approximately 100 million dollars is required in a single coastal district. In addition to this cost is the fact that the bridges in the sample have an average life of 30 years and therefore would have to be replaced twice in a normal 75 year design life. Table 2.5 is a sample of additional districts where the adverse combinations will certainly lead to high replacement costs.

To further understand the economic impact, the entire State of Texas has a current bridge replacement cost due to substructure deterioration of **\$2,193, 493,000**. This figure is based on all of the multipliers and equations given above and the data in Table 2.4.

2.4 Field Trip Investigations. The primary purpose of dividing the state into four geographic regions was to reduce the amount of work that is required to adequately field

review the districts. Once the four geographic regions were established a representative



ADT

- 10,001 - 50,000
- 4,001 - 10,000
- 2,001 - 4,000
- 0 - 2,000

Figure 2.3: Average ADT Counts by District

district was selected from each region. The four geographic regions along with their respective districts are given in Table 2.6.

Table 2.5: Additional Districts and Their Adverse Conditions

District	Detrimental Aspects
Amarillo (4)	Low mean age of structure (30.6) High ADT (12,390) High average number of spans (9)
Beaumont (20)	Low mean age of structure (36.9) High ADT (14,671) High average number of spans (11)
Dallas (18)	Low mean age of structure (34.4) High ADT (24,406) High average number of spans (10)
Odessa (6)	Low mean age of structure (34.4) Moderate ADT (5,133) High average number of spans (12)

Table 2.6: Districts and Their Respective Regions

District	Geographic Region the District Represents
Amarillo	West Texas
Austin	Central Texas
Corpus Christi	The Coastal Area of Texas
Paris	Northeast Texas

Three of the four districts shown were visited and a significant amount of data was acquired from these districts, Amarillo, Corpus Christi and Austin. Due to the time constraints of the project the Paris district has not been visited at the time of this thesis.

2.4.1 The Amarillo District. The Amarillo district represents the West Texas region. This region has severe corrosive attacks on this district's bridge substructures from de-icing salts. The district currently has the responsibility for 724 on-system bridges. Of the 724 on-system bridges in Amarillo, 114 of these structures have a substructure rating of 6, 32 structures have a substructure of 5 and 14 have a rating of 4 or below. A rating of 4 is a substructure in “ poor condition where deterioration has significantly affected the structural capacity.”

The longevity of this particular sample is significant. The breakdown of when these structures listed in the paragraph above were built is given in Table 2.7.

Table 2.7: Approximate Year Built of Sample in Amarillo

Number of Bridges	Age of Structure
8	Built after 1980
9	Built after 1970
81	Built after 1960
62	Earlier than 1960
160 Bridges	Total

As mentioned previously, the longevity of substructures that are significantly reduced are primarily from the West Texas region or the Coastal region. The sample

from the Amarillo district is very representative of the West Texas region. To take a micro view of the corrosion phenomena in this region a field visit was conducted for several structures. These structures were either visited or discussed in detail with the BRINSAP personnel of this district. A listing of the structures reviewed is given in Table 2.8.

The trends in the district which are representative of the western region as a whole are significant. The area that is impacted the most is the substructure directly under an open joint. This area is prone to several freeze thaw cycles on top of the bent caps over the course of a single winter. Generally the cap will exhibit top and side splitting of the top reinforcement.

Table 2.8: Individual Projects Reviewed in the Amarillo District

Structure #	Year Built	Subs. Rating	Bridge Type	Superstruct. Rating	ADT
149	1984	5	Pre-stressed Conc. Girder	8	4750
1	1971	5	Precast Conc.	5	3900
26	1962	4	Pan	5	3650
2	1962	4	Steel I-Beam	6	5800
10	1932/1948 *	4	Conc. Girder	4	3650
7	1957	4	Pan Girder	5	170
5	1977	6	Pre-stressed Conc. Girder.	8	4000
39	1966	4	Pre-stressed Conc. Girder	6	30700

This is illustrated in Figure 2.4. In this photograph of a bent cap built in 1984 the cracking of the bent cap is primarily parallel to the direction of the main reinforcement.

Notice the leaching of calcium carbonate above the bent cap on the bottom of the slab. This leaching is indicative of a construction joint.



Figure 2.4: Top and Side Splitting of Upper Reinforcement in Bent Cap (Amarillo)

As the structure begins to age the chloride penetration migrates to the lower portion of the cap and the entire cap becomes cracked and in need of replacement. The next photograph is an older structure where the corrosion has become more pronounced. This is evident in Figure 2.5. The structure on US 87 was built in 1962 and therefore is thirty-four years old. Note the significant amount of damage from the chloride penetration in this structure.

Of particular interest to this report are the columns in the Amarillo District. Chloride migration into the columns can occur from three principal methods.

1. The water from the bridge deck runs through the open joint down onto the cap and then travels the length of the column as the water runs to the ground.
2. Accumulation of plowed snow from the roadway is piled against the column below the structure.
3. Several bridges have been constructed with the beams bearing directly on the columns. This leads to the same corrosive attack that was illustrated in the bent caps with the attack occurring on the top of the column.



Figure 2.5: Severe Deterioration of an Amarillo Bent Cap

Figure 2.6 illustrates the corrosive attack of single columns directly supporting a beam and under an open joint.



Figure 2.6: Single Column Directly under a Construction Joint in Amarillo.

The adverse affects of snow accumulations pushed onto the bridge columns can be seen in Figure 2.7. The field studies in Amarillo offered significant insight to the transportation of chloride ions into the structural member. The project shown in Figure 2.7 is two overpasses on Interstate 40. Interstate 40 has a high volume of traffic with an ADT count of 1850 cars per day. Table 2.9 illustrates the chloride samples taken from this substructure by a concrete powder test performed by TxDOT.

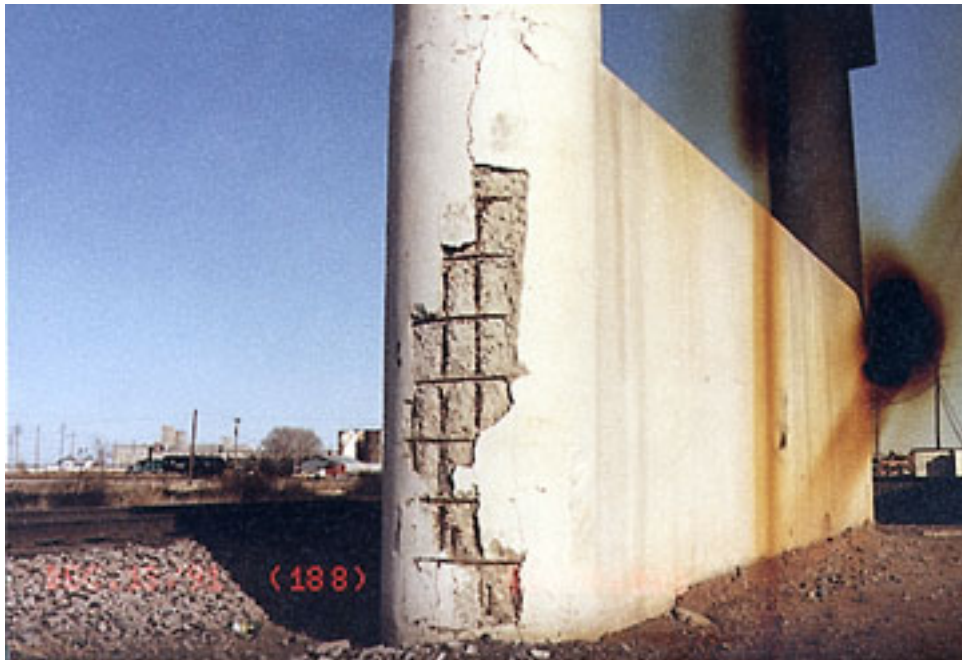


Figure 2.7: Deterioration of Columns Due to Salt Laden Snow Piled against the Column

Table 2.9: Chloride powder test on columns, Project 275-1-38 Amarillo (IH 40)

Sample	Depth	%Cl	PPM	Lbs./Cu. Yd.
1	0"-1"	.08	755	3.0
2	1"-2"	.11	1,058	4.2
3	0"-1"	.66	6,581	26.3
4	1"-2"	.33	3,270	13.1
5	0"-1"	.14	1,381	5.5
6	1"-2"	.14	1,440	5.8
Sample	Location		Span	Distance
1 & 2	Bent #2			
3 & 4	Bent #3		Col. #3	2' from Top
5 & 6	Bent #3		Col. #3	4' from Gnd

The most significant aspect from these tests is the concentration of the chloride ions some distance from the top of the column and the bottom of the column. Consider samples 5 & 6, located four feet from the ground. In this area the concentration is higher closer to the reinforcement and is concentrated above the height where salt laden snow would accumulate. This example can be found repeatedly in Amarillo. These observations show that there is water movement within the pore structure of the concrete and suggests capillary action.

The durability attacks in the substructure members in several Amarillo bridges are significant. The most prevalent attacks occur under open joints between spans. However, there are also corrosion indications under and near construction joints. Finally, there is enough evidence to suggest capillary rise or “wicking” in bridge columns where salt laden snow has accumulated against the bridge columns.

2.4.2 The Corpus Christi District. The Corpus Christi District was selected as a representative sample of the coastal area. The primary area of concern is structures located immediately adjacent to the Gulf of Mexico. There are 25 on-system bridges in this district with a substructure rating of five (5) or below. This sample of deficient bridges is approximately 2% of the total of on-system bridges in this district. This 2% is primarily on the coast.

The durability problems are similar in nature to the Amarillo District. The chloride egress penetrates from wave and ocean spray onto the bent caps. The horizontal splitting of the upper and lower reinforcement is evident in Figure 2.8.



Figure 2.8: Horizontal Splitting of the Upper and Lower Reinforcement in a Typical Bent Cap

The coastal substructures not only suffer from bent cap durability problems but in the columns and piling as well. The columns have the same type of attack as the columns in the West Texas region. The columns suffer from face splitting in the longitudinal direction. This face splitting is illustrated in Figure 2.9.



Figure 2.9: Face Splitting of a Bridge Column in Corpus Christi

The penetration of the chloride ions occurs above the water line where a fresh supply of oxygen is readily available. The question that remains is how much of the chloride penetration comes from tidal action and spray versus how much comes from

capillary rise in the pore structure. Mirsa and Uomoto have documented the question of capillary rise in the pore structure of the concrete in a paper entitled, “Reinforcement Corrosion under Simultaneous Diverse Exposure Conditions.” (15) Mirsa and Uotomo state that “...in this case by capillary action, plays a vital role in the transport of chlorides within the concrete.” This capillary action is a significant aspect considered in this thesis and is considered in the development of the column models. The author suggests that capillary action exists in Texas Bridge Columns and will attempt to model the phenomena in the ½ scale models presented in Chapter 3.

2.4.3 The Austin District. The Austin District was selected as the representative district of the central region. Due in large part to the weather and the environment, very little corrosion occurs among these districts. The exception to this rule is Odessa. The Odessa District is home to several rivers with a very high saline content in the water. As with the West Texas and Coastal environments this leads to significant corrosion in the substructure from chloride egress in the concrete.

Excluding the river areas of the Odessa district the Central Texas Area has very little corrosion among its substructures. The BRINSAP report shows 48 structures with a substructure rating of 5 or below. The actual number of structures with significant corrosive attack was 7. This number was determined through field investigation and subsequent meetings with Mr. Jeff Howell, P.E. the BRINSAP coordinator for this district. Of the seven bridges with significant substructure corrosion only one structure was built after 1950. The remaining bridge’s low ratings stem from foundation settlement, impact damage and bridge scour.

2.5 Future BRINSAP Studies. Presented in this report are the rudimentary statistics

required to present a basic trend in current TxDOT bridges as these bridges pertain to substructure condition. The question as to whether or not Texas Bridge substructures have a durability concern has been answered. To further analyze the extent, severity, cause and propagation, the database needs to be subdivided further. Throughout the state different districts have used various corrosion prevention techniques. These techniques could be incorporated into the BRINSAP data base as a comparison to structures built in the same geographical region with a similar environment.

There are several flaws with the accuracy of the first sample. One such flaw or defect is that the substructure material is not certain to be concrete. In other words some of the bridge substructures in the sample may be either steel or timber. Items in the current BRINSAP code allow us to remedy this aspect. However, there is not a category to subdivide substructures into prestressed, cast-in-place or post-tensioned and this could produce significant findings. Certainly the ability of the current program is such that all of these recommendations could be adopted with little effort. As technology in bridge and in particular substructure construction changes, the tools for recording deterioration need to be refined to reflect the performance of this technology. This effort will help close the gap between the design service life and the actual service life of the substructures in Texas.

Chapter 3 Test Program

3.1 Introduction. To simulate the Texas Bridge columns and to examine durability of bridge columns in a long-term exposure environment, a long-term exposure test must be established. This test should replicate ‘in-field’ conditions such as applied dead load, axial load, and moment. The column models should be subjected to the Standard Half-Cell Corrosion Test, in accordance with ASTM C876 as well as the current linear polarization testing techniques. These tests will determine the rate and extent of corrosion activity. Although these tests are not specifically designed for post-tensioning applications they can be readily adapted for such purposes.

The corrosion of reinforcing steel proceeds at a much faster rate in the presence of chloride ions. To determine the extent of chloride ion egress into the column, a powder test should be conducted on the columns in conjunction with AASHTO T260 and ASTM C114 standards.

3.2 Specimen Design. The long-term exposure test is designed to accurately model a TxDOT standard 36-inch diameter column. To achieve this objective a half-scale model was designed, proportioned and detailed according to typical TxDOT practice. To expose the concrete scale model columns to a long term exposure condition a testing scheme was needed.

To subject the base of the columns to long term exposure conditions a trough was chosen. This trough or foundation allowed one to simulate pier cap column interface connections. The foundation had to be developed such that the foundation itself would not corrode. In addition, the foundation had to be designed to resist the imposed dead loads applied to the columns.

The measure of corrosion, as suggested earlier, can be accomplished in several ways. This project chose linear polarization, half-cell test, chloride powder samples and

autopsy of some specimens half way through the test.

3.2.1 Specimen Variables. Post-tensioned concrete is comprised of many variables. The prominent variables evaluated in this thesis are the post-tensioned tendons, end anchorage, ductwork, grout, concrete type, load type and connection type. The actual specimen types are based on four principal comparisons:

1. Performance of post-tensioning versus conventional pile cap connection for long term exposure without applied service loading.
2. Performance of post-tensioning versus pile cap connection for long term exposure under service loads.
3. Performance of low permeable concrete versus TxDOT Class C under service loading and without applied service loads.
4. In addition, other group comparisons, such as comparison of performance of no joint specimens under service load versus low permeable concrete.

In these comparisons ‘performance’ is defined as the specimens ability to withstand the progression of corrosion including the time and method of corrosion which includes ‘wicking’ effects. These comparisons fall into five distinct categories. These categories are:

Group 1: Connection type with no service load applied

Class C + TxDOT Doweled Connection + $P_{\text{service}} = 0$ + $M_{\text{service}} = 0$

Class C + Post-tensioned Connection + $P_{\text{service}} = 0$ + $M_{\text{service}} = 0$

Class C + No Joint + $P_{\text{service}} = 0$ + $M_{\text{service}} = 0$

Group 2: Connection type with service load applied

Class C + TxDOT Doweled Connection + $P_{\text{service}} = 75$ kips + $M_{\text{service}} = 225$ k-in.

Class C + Post-tensioned Connection + $P_{\text{service}} = 75$ kips + $M_{\text{service}} = 225$ k-in.

Class C + No Joint + $P_{\text{service}} = 75$ kips + $M_{\text{service}} = 225$ k-in.

Group 3: Affects of low permeable concrete

35% Fly Ash + TxDOT Doweled Conn. + $P_{\text{service}} = 75 \text{ kips} + M_{\text{service}} = 225 \text{ k-in.}$

35% Fly Ash + Post-tensioned Connection + $P_{\text{service}} = 75 \text{ kips} + M_{\text{service}} = 225 \text{ k-}$

in.

Group 4: Affects of epoxy coated vs. galvanized vs. conventional tendons

Class C + P/T Connection (epoxy) + $P_{\text{service}} = 75 \text{ kips} + M_{\text{service}} = 225 \text{ k-in.}$

Class C + P/T Connection (galvanized) + $P_{\text{service}} = 75 \text{ kips} + M_{\text{service}} = 225 \text{ k-in.}$

Class C + P/T Connection (black) + $P_{\text{service}} = 75 \text{ kips} + M_{\text{service}} = 225 \text{ k-in.}$

Group 5: Affects of post-tensioning duct; galvanized versus plastic

Class C + P/T Connection (plastic duct) + $P_{\text{service}} = 75 \text{ kips} + M_{\text{service}} = 225 \text{ k-in.}$

Class C + P/T Connection (galv. duct)+ $P_{\text{service}} = 75 \text{ kips} + M_{\text{service}} = 225 \text{ k-in.}$

Several variables in the post tensioning system were not considered in this long-term exposure test. One of the more prominent variables is the grout in the duct. This variable was covered in the scope of this research project under the accelerated grout testing performed by Brad Koester and Andrea Schokker. The grout chosen for this test complied with the 1993 TxDOT specifications and the water/cement ratio was held to 0.44.

The concrete permeability is a significant variable in this test. There are an endless amount of possibilities of concrete mix designs. Once again, the concrete mix design chosen was in compliance with TxDOT specifications, specifically Class C concrete. Therefore, Class C concrete became the control variable and was modified to decrease the permeability by adding the maximum amount of Class C (TxDOT Class B) fly ash. The maximum amount allowed by TxDOT specifications is 35%. The duct that houses the tendons is a significant variable. The plastic duct is essentially inert, while the galvanized duct could possibly cause galvanic corrosion or cause a stray current. The geometry and the duct concrete interface will be held constant throughout the test.

3.2.2 Development of the column model. In bridge columns, the primary loading condition is axial loading applied by dead load. Granted, the live load from traffic is transferred through the beams, then through the cap and into the column but these loads are generally not as large as the dead loads. The design of reinforced concrete columns can be very complicated. The analysis of this member subjected to axial load and moment is difficult and the accurate determination of the amount of bending is dependent upon second order analysis. To insure adequate design TxDOT limits the dead load service level stresses at 22 ksi.

To accurately model the service load condition a study of several bridges was conducted to determine an average service load. A bridge in Dallas County with two lanes of traffic and full shoulders was selected. The average span length was 100 feet in length and the superstructure was supported by a three-column bent with 30 inch diameter columns. The service load moment and axial load are based on AASHTO HS-20 loading conditions. The moment and axial load on these columns of this bridge structure were as follows:

Column 1

$$M_{\text{service}} = 107 \text{ kip feet.}$$

$$P_{\text{service}} = 386 \text{ kips}$$

Column 3

$$M_{\text{service}} = 87 \text{ kip feet}$$

$$P_{\text{service}} = 209 \text{ kips.}$$

The relationship to scale the moment and the axial force can be derived from the interaction diagram of a non-slender column. If the eccentricity of the axial force is held

constant, then the 3/5 scale modeled column can be derived from the relationship:

$$P_{N30} / A_{g30} = P_{N18} / A_{g18} \text{ and } A_g \text{ can be expressed in terms of diameter as } \pi(d^2/4).$$

Solving for the scaled axial force in the 18" column is given as:

$$\{\pi(d_{18}^2/4)/\pi(d_{30}^2/4)\}P_{N30} = P_{N18} \quad (3-1)$$

The moment can be derived from the constant slope and the known axial force from the expression $P_N * e = M_N$. The final concern in developing the applied service load (P_{N18}) and the applied service moment (M_{N18}) was decompression at the joint. Since the typical TxDOT Bridge is founded on drilled shafts, decompression is not relevant for the Prototype Bridge from which the scaled model in this thesis is developed. The scaled models have a joint connection and the research group agreed that decompression at the joint would flaw the test. Elastic decompression with a service load of 100 kips was calculated at 225 k-in. Using the relationship with zero stress at the extreme concrete fiber of the 18-inch column section, the following relationship can be determined:

$$F_{bot}=0; \text{ and } 0=P/A_{tr}-M/S_{tr} \quad (3-2)$$

where P_{serv} is the 100 kip service load developed above. A_{tr} represents the transformed area of the column. Since the column is completely in compression, all of the reinforcement is in compression and the area is valid. The AASHTO Highway Bridge Code and the scale model of the bridge prototype referenced earlier drive the reinforcement. The required vertical reinforcement is 6-#6 bars, which represents an area of steel equal to 2.64 square inches. The concrete 28-day design compressive strength is 3600 psi based on the TxDOT Class C requirements. The Modulus value of

the steel is chosen as 29,000 ksi. Therefore the modular ratio, n , is 8.48.

3.3 Materials. The materials selected for this thesis are in conformance with TxDOT specifications. The control variables involved the reinforcement, the post-tensioned bars, the concrete, and the post-tension ductwork. The passive reinforcement and the grout used in the post-tension ducts were held constant.

The foundation base was designed with 5000 psi. concrete. Fly ash was used as a replacement for part of the cement in the base concrete. A 30 % by volume substitution was used for the cement content. The high performance concrete was used to insure that the base structure did not corrode prior to the test specimens. In addition to the base structure's low permeability, the base structure also employed epoxy reinforcement with a 3-inch concrete cover over the reinforcement at the top of the structure. To provide additional insurance against chloride intrusion, a two-coat epoxy paint system was painted on the inside bottom and sides of the trough after the columns were cast. Care was taken to ensure that the column–foundation interface was not painted so that the actual conditions at the joint could be observed.

3.3.1 Concrete. The one element that is exposed to all of nature's forces in concrete bridges is the concrete itself. In a corrosive environment, without proper concrete, the bridge will surely experience some form of corrosion. TxDOT specifications provide 13 classes of concrete for all of the bridges found in Texas. The bridge substructural components are currently specified to be Class "C" concrete. Prior to 1972 (14) all bridge substructure components were Class A. Class A and Class C are very similar in specification. The argument made is that the change in technology over the years from Class A concrete to Class C concrete will increase the longevity of Texas Bridges substructural components. The permeability of concrete is affected by water-cement ratio, the presence of concrete admixtures, sample age, air void system, degree of aggregate consolidation and type of curing. (3). The single most important factor is time. ASTM states, " most concretes, if cured properly, become progressively and

significantly less permeable.” If the before mentioned argument is valid, then one would have to accept concrete variability, and in particular, concrete permeability as the single most important component in the corrosion of the bridge’s substructure.

The current Class C concrete, as specified, has a relatively high water to cement ratio. This ratio, w/c, is specified at 0.53. In order to compare the relative effect of the water/cement ratio and other variables of TxDOT Class C concrete, the research team conducted a series of permeability tests from samples of TxDOT concrete currently being used on TxDOT bridge substructures. Samples were selected from the Austin District as well as from regions across the state as defined earlier in this thesis. The permeability testing method selected was the AASHTO T277 Rapid Chloride Ion Permeability Test. This test is the equivalent of the American Society of Testing Materials (ASTM) test designation, C 1202-91.

This test method covers the determination of the electrical conductance of concrete to provide an indication of the concrete’s resistance to chloride ion penetration (4). In most cases to date, electrical conductance has shown good correlation to concrete ponding tests. Recently, some new concrete diffusion tests have not correlated well. In the past 10 years the measure of permeability has been a subject of continued debate. To date, the subject is still inconclusive. The research team decided to use the current ASTM test until another test is adopted.

The test method consists of monitoring the amount of electrical current passed through a 2-inch thick slice of a concrete cylinder during a 6-hour duration. A potential difference of 60 V DC is maintained across both ends of the specimen, one of which is immersed in a sodium chloride solution, the other in a sodium hydroxide solution. The total charge passed in coulombs has been found to be related to the resistance of the specimen to chloride ion penetration (astm). ASTM categorizes the permeability of the concrete into 4 distinct categories. The categories are given in Table 3.1, below as:

Table 3.1: Chloride Ion Penetrability Based on Charge Passed (1)

<i>Charge Passed (coulombs)</i>	<i>Chloride Ion Penetrability</i>
>4,000	High
2,000-4,000	Moderate
1,000-2,000	Low
100-1,000	Very Low
<100	Negligible

A complete description of the AASHTO and ASTM test is given in Appendix A. Mr. John Myers, P.E., a doctoral candidate in the materials group of The University of Texas at Austin conducted the permeability tests in accordance with the AASHTO test method.

Locally, three ready mix companies supplied two cylinder samples of TxDOT Class C concrete for permeability testing. The companies represented were Alamo Products, Capitol Aggregates, and Centex Materials. A complete description of the mix designs for each firm is shown in Table 3.2.

Table 3.2: Local TxDOT Class C Mix Designs Tested for Permeability by AASHTO 277

Supplier	Date Cast	Temp.	Design #	Slump
<i>Alamo Products</i>	12-Sep-95	85	TCAR/FA	4.25"
	% Ash	% Cement	% Air	Water/ Cement
	27.5	72.5	6.7	0.475

Mix Design
(per cubic yard)

Course Aggregate	1839 lbs.	1" Crushed Stone
Fine Aggregate	1161 lbs.	TXI (Green Pit)
Fine Aggregate	lbs.	
Cement	409 lbs.	Alamo Type I
Fly Ash	128 lbs.	Monex La
		Grange
Air Additive	3.48 grams	Master Builders
		AE90
Retarder	27 oz.	Pozz 300R

Supplier	Date Cast	Temp.	Design #	Slump
Capitol Aggregates	12-Sep-95	91° F	148	2.75
	% Ash	% Cement	% Air	Water/ Cement
	27.5	72.5	3.5	0.443

			Mix Design (per cubic yard)
Course Aggregate	1855 lbs.		Grade 2 River Rock
Fine Aggregate	1245 lbs.		****
Fine Aggregate	lbs.		
Cement	409 lbs.		Capitol Type I
Fly Ash	133 lbs.		Monex
			LaGrange
Air Additive	**	grams	Master Builders
			AE90
Retarder	20 oz.		Pozz 300R

Supplier	Date Cast	Temp.	Design #	Slump
Centex Materials	12-Sep-95	94° F	822	4.5
	% Ash	% Cement	% Air	Water/ Cement
	27.5	72.5	6.7	0.475

Mix Design
(per cubic

Course Aggregate	1750 lbs.	yard)
Fine Aggregate	835 lbs.	Southern
		Materials
Fine Aggregate	351 lbs.	Texas
		Crushed
		Stone
Cement	406 lbs.	Texas Lehigh
		Type I
Fly Ash	158 lbs.	Monex
		LaGrange
Air Additive	3.4 grams	Master
		Builders
		AE90
Retarder	** oz.	Master
		Builders
		100XR

The three mix designs have similar characteristics. The percent fly ash is measured by a percentage of the volume, not the weight. The percent fly ash is identical in all three mix designs. In addition, the weight of cement is within 3 lbs, in all of the mixes. Finally, the water-cement ratio is well within the TxDOT Specifications for a Class C mix design. The test was in fact localized and the sample size too small to have conclusive results. The significant point is the great deal of variability between various concrete suppliers even with specific mix design parameters. A given 6-inch x 12-inch cylinder yields three slices of concrete to be tested. Therefore, 6 tests were run for each concrete supplier. The permeability for the AASHTO 277 test is measured in coulombs. The averaged results for the specimens from the three local concrete vendors are given in Table 3.3..

Table 3.3: Results of AASHTO Permeability Tests

<i>Concrete Mix Supplier</i>	<i>Average Permeability (coulombs)</i>	<i>AASHTO Classification</i>
Alamo Products	2835	Moderate

Capitol Aggregates	1735	Low
Centex Materials	3020	Moderate

The project selected Capitol Aggregate as the vendor for all of the column specimen concrete. The results for the three mixes supplied have a large amount of variability with a swing of 1,285 coulombs passed. This simple test illustrates the amount of variability in the specified mix design even in a localized region. The TxDOT durability problems in the substructure components can not be resolved with the concrete design alone. The protection schemes for the reinforcement in the substructure components will certainly have to extend beyond the concrete.

3.3.2 Post-Tension Steel. Today there is a wide variety of mechanical post-tensioning methods available. TxDOT currently employs both strands and bars in their post-tension applications. The 3/5 scale model evaluated both methods. The strands have a higher elongation than do high-tensioned bars. Therefore, the bars were an obvious choice. The integrity of the model is preserved in the fact that the majority of the bridge columns cast are considered short relative to their gross area. This feature is a typical designer's choice to eliminate slenderness affects. Considering these factors, the high-tensioned bar system from Dywidag-Systems International was selected.

The determination of the post-tension (P/T) force was based on the increased moment capacity. Figure 3.1 represents a column interaction diagram with conventional passive reinforcement, with post-tensioning bars only and finally with both passive and post-tension reinforcement. The most significant aspect, from a design point of view, is the increase in moment capacity in the tension zone of the interaction diagram, thus increasing the ductile capacity of the column. In addition to the increase in ductility is the decrease in crack width. The reduction in crack width is minimized in this model due to the amount of service load applied to the member. Given this fact, the post-tension steel will close any shrinkage cracking, which may develop in the column from

thermal expansion after casting.

<Interaction Diagram ACAD DRAWING>

Figure 3.1: Interaction Diagram for the 18” Column Specimen

To determine the amount of post-tensioning required, the gross area was considered with respect to the use of a full scale TxDOT Bridge Column. The ‘x’ notation in Figure 3.1 represents the scaled service load and moment location on the interaction diagram. Typically, TxDOT’s column designs are conservative. Based on this information, the minimum post-tensioned bar size of 5/8” was selected. To apply uniform P/T force over the gross section of the column, four bars were selected. Figure 3.2 illustrates the plan section of the column with the location of the passive

reinforcement as well as the post-tensioned bars. The P/T force applied was selected to be $0.6 \cdot f_{pu} \cdot A_s$. Where the ultimate material stress, f_{pu} , is 157 ksi, the area of steel, A_s , is 0.28 square inches. Therefore the applied force is approximately 26.4 kips/bar.

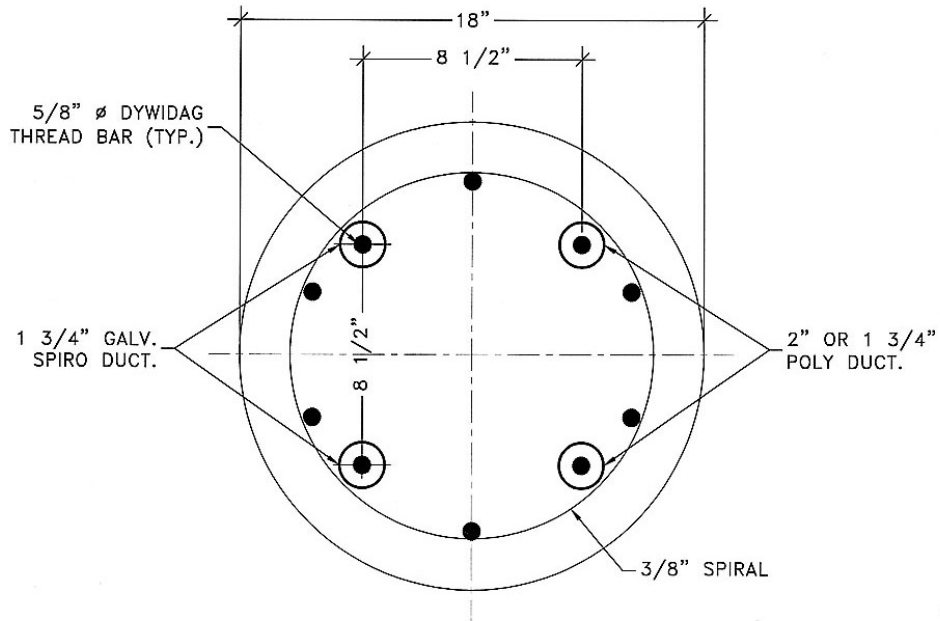


Figure 3.2: Section View, in Plan, with the Location of the P/T Bars

To be consistent with TxDOT design the effective post-tension force after losses was calculated in accordance with AASHTO 9.16.2.1. The loss of stress is determined by:

$$\Delta f_s = SH + ES + CR_c + CR_s \quad (3-3)$$

Where SH is equal to the loss of stress due to shrinkage of the concrete, ES is the

elastic shorting of the concrete, CRc is the loss due to the creep of the concrete and CRs is the loss due to the relaxation of the steel. The first loss given, shrinkage is influenced by several factors. Shrinkage is time dependent and is most dramatically affected by humidity, the volume-to-surface ratio and the time from moist curing to post-tensioning (17). The loss due to shrinkage of the concrete is determined by:

$$SH = 8.2 \times 10^{-6} K_{sh} E_s \{1 - 0.06V/S\} (100 - RH) \quad (3-4)$$

Where: E_s = Modulus of Elasticity of the Steel

K_{sh} = Shrinkage Loss Coefficient

V/S = Volume to Surface ratio

RH = Relative Humidity

Elastic shortening loss is due to the shortening of the concrete after the post tension force is applied to the member. In the case of a single bar or tendon, the concrete shortens as the bar is tensioned. The force is then measured after the concrete has shortened, therefore; no loss needs to be accounted for. With multiple strands or tendons, the first tendon or bar experiences the loss when force is applied to the next tendon or bar. In order to average the losses among the first and subsequent bars the AASHTO code allows a value of half of the loss for the subsequent bars that the first bar experiences. Thus the 0.5 factor for the elastic shortening equation is shown below.

$$ES = 0.5(E_s/E_{ci})f_{cir} \quad (3-5)$$

Where E_s is the modulus for the post tension bar, E_{ci} is the modulus for the concrete and f_{cir} is the stress in the concrete at the level of steel due to the applied P/T force.

The last two factors in Equation 3-3 are time-dependent losses. The first, creep of the concrete, is due to additional strain in the concrete experienced under a sustained

load. In bridge columns, the dead loads are a large percentage of the load and are the single most important contribution to the calculation of creep in the concrete. The AASHTO concrete creep equation for determining this loss is given by:

$$CRc = 12f_{cir} - 7 f_{cds} \quad (3-6)$$

Where as before f_{cir} is the concrete stress at the level of steel and f_{cds} is the stress in the concrete at the center of gravity of the tendons due to all super-imposed dead loads that are applied to the member after stressing. (17)

The last component of the equation is the time dependent loss due to relaxation of the steel. Tests with steel bars and strands over a long period of time have demonstrated that the force will decrease (17). The amount of loss is dependent on the ratio of f_{pi} over f_{py} where f_{pi} is the initial stress in the post-tension steel after stressing and f_{py} is the yield stress. AASHTO has, as do many codes, a constant loss which is derived from a table. The loss due to relaxation for the post-tension bars used in this experiment is given from AASHTO as 3.0 ksi. The loss due to concrete shrinkage is 4.6 ksi. As calculated from Equation 3-4, elastic shortening is determined from Equation 3-3 to be 1.7 ksi. Finally, the creep of the concrete was calculated from equation 3-6 as 2.0 ksi. The total loss in the post-tensioning is 11.3 ksi. Therefore, the loss in force after multiplying the area of steel by the total loss in stress is 3.16 kips/ bar. This loss will be accounted for in stressing the P/T bars. Figure 3.3 illustrates the complete post-tension assembly in section.

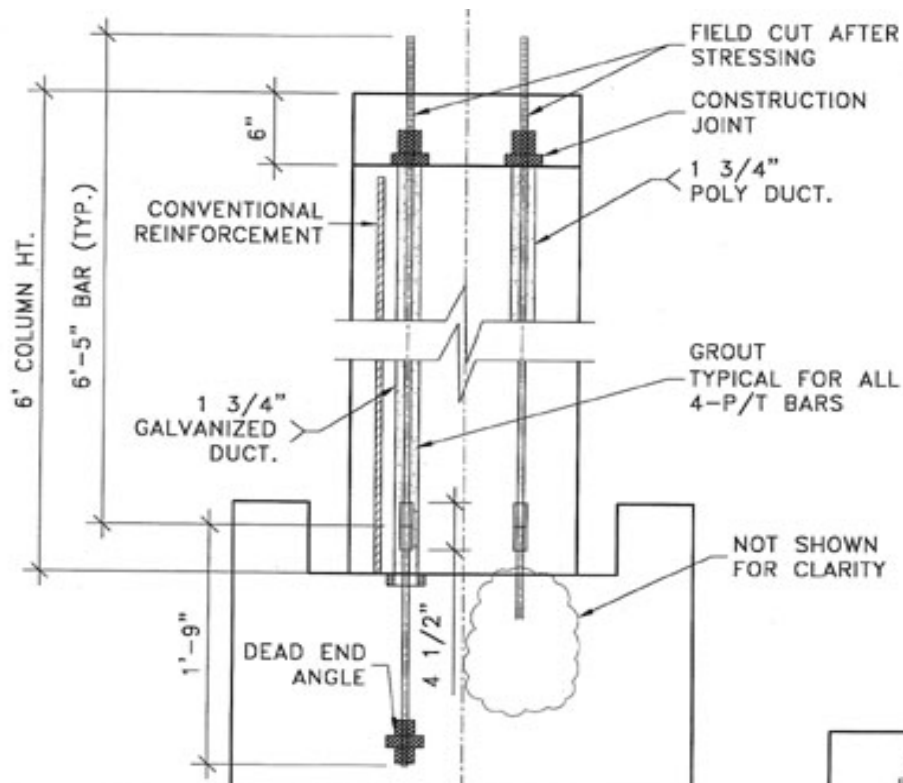


Figure 3.3: Section of the Column P/T Assembly

Inspection of Figure 3.3 reveals two areas of concern for the design engineer. The first is the column-foundation interface. The bars would be dead-ended into the foundation, pass through the column-foundation plane and be coupled near the bottom of the column. This detail would provide an opportunity for chloride penetration at the column specimen / foundation interface. A similar detail is found in TxDOT column-to-tie cap connections and has a great potential for corrosion, particularly if the column is subjected to moment where decompression at the joint could occur.

A detail was designed to embed the duct into the foundation at a depth of 1-1/2"

below the typical interface plane. A neoprene hard rubber gasket was designed to fit neatly in the embedment. Figure 3.4 depicts this gasket after the foundation was cast.

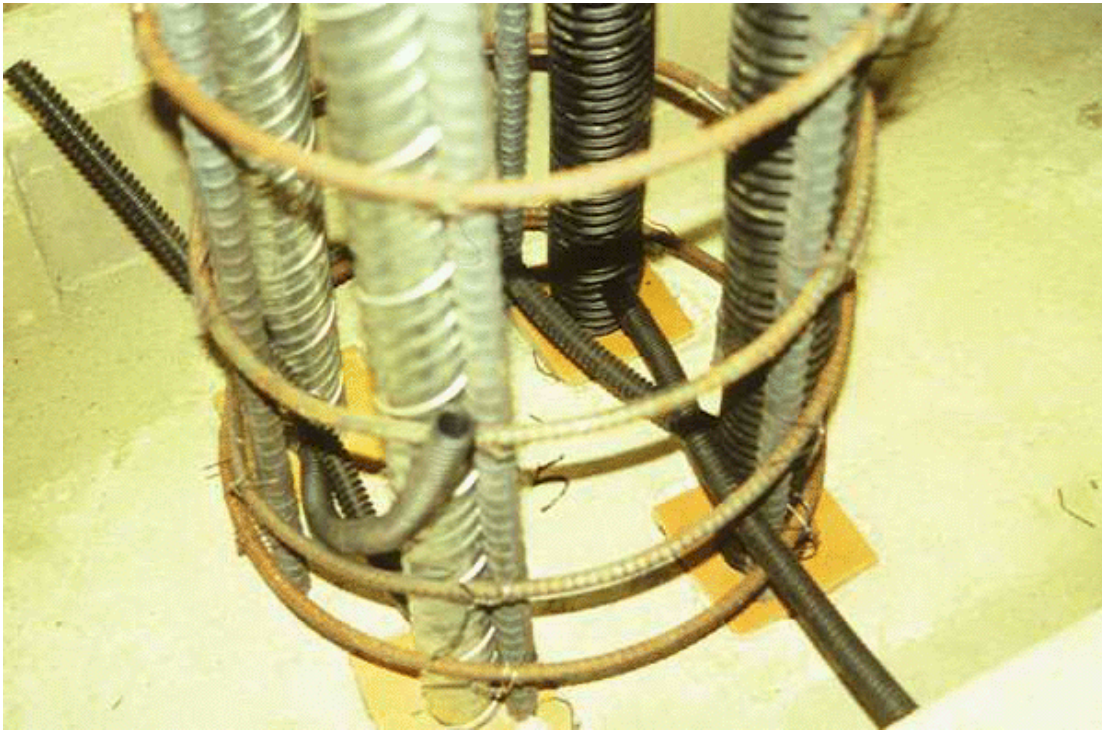


Figure 3.4: Installation of the Rubber Gasket at the Column-Foundation Interface

After the columns are cast and cured the P/T bars will be stressed. As shown in Figure 3.3 the P/T bars are stressed and then cut. Finally a closure pour is required to "cap" the column. Typically, this closure pour would be completed in a bridge structure with another component such as a bent cap. The simulated loading condition required the research team to "cap" the column as shown in Figure 3.3. The actual stressing will be presented in Section 3.4.6

3.3.3 Reinforcing Steel. The column specimens are no different than their full-scale prototype columns when considering passive reinforcement. The reinforcement

required is detailed for a standard 18-inch column. The column specimen design required 6-#6 vertical members. The vertical members selected are ASTM A706 Grade 60, (60 ksi) steel. Spiral reinforcement is employed to hold the cage together at 6 inches-on-center (o.c.) with a full turn on the top and the bottom. Figure 3.4 illustrates the column section as well as their relative location on the foundation. All of the passive reinforcement used was tested in accordance with TxDOT's Standard Specifications for Construction of Highways, Streets, and Bridges Item 440. The AASHTO cover requirements for bridge columns required a 1-1/2" side clear cover. The gage is tied at each intersection with the spiral to insure compliance with TxDOT specifications. This cover was maintained with the use of plastic-tipped chairs. These chairs meet the TxDOT requirements and are the industry standard. Individual chairs were placed at a maximum of three-foot on-center.

To meet the criteria established earlier in this thesis, three types of connections had to be established. The first is no connection, or a column without a foundation connection. This "no connection" occurs in Column Specimens 5, 6, 8 and 10. This condition is used to simulate a foundation connection where the foundation would be at a distance below the water line. A single epoxy bar, # 5, is used as a center pin dowel to hold the column in place. The passive reinforcement is held at a clear distance of 2-inches to insure no corrosion occurs at the bottom of the column. The second joint is a representation of a doveled joint typically found at a column-to-pier cap connection. The connection to transfer a potential moment is detailed using 6-# 6 bars with a 90° hook into the foundation. The development length required beyond the foundation is 24 inches. Each dowel is tied with a "double wrap" at the top and the bottom of the gage. The vertical members rest on top of the foundation. The passive reinforcement gage in the column specimens is part of the column design, but should not interact with any of the post-tensioning. Great care was taken in the construction of the specimens so that the P/T bars did not come into contact with the passive reinforcement.

The final type of connection is the post-tensioned connection. The P/T bars are

responsible for the moment transfer to the pier cap. This type of connection improves the cover distance without sacrificing or compromising the reinforcement. Studies have demonstrated a point of diminishing return when reducing cover as the passive reinforcement is not close enough to the surface to control the crack width. By allowing the P/T bars to carry the connection, the passive reinforcement's cover is still 1-1/2" away from the surface, a distance that controls crack widths well. This hypothesis will be tested during the long-term exposure of the specimens.

3.3.4 PE Duct. One of the many comparisons the long term exposure testing will review is the comparison between post tension ducts. A matrix of two types of ducts was coupled with three types of P/T bars. The types of bars are black, galvanized and epoxy coated. The columns receiving the post-tension application are column numbers 2, 5, 7, 9 and 10. Table 3.4 displays the columns and their duct-P/T bar combination.

Table 3.4: Matrix Combination of Duct and P/T Bars

Duct\Bar	Black P/T Bar	Epoxy P/T Bar	Galvanized P/T Bar
Galvanized Duct	Column 5	Column 9	Column 10
PE Duct	Column 5	Column 9	Column 10

The matrix in table 3.4 illustrated the various combinations of duct and P/T bar. The rest of the variable for columns 5, 9 and 10 are uniform. Each of the columns have an applied load, service moment and each is a Class C concrete. This project will hope to determine which of the combinations, all experiencing the same exposure conditions, will provide the best resistance to corrosion.

To protect the post-tensioning bars from the corrosive effects of the environment, several variables must be examined. As explained previously, the concrete cover and it's permeability is just one of the before mentioned variables that must be considered.

Beyond the concrete and its cover, is the duct that encloses the post-tensioned bars and the grout that fills the duct. The polyvinyl-ethylene (PE) plastic is the manufacturer's recommended duct in corrosive environments. The TxDOT Specifications require the duct to be “ *sufficiently rigid to withstand placement of concrete, grouting and construction loads without damage or excessive deformation, while remaining watertight...*” In addition, the PE duct must be in accordance with ASTM Designation D3350, and D2239, D2447, or D3035, with cell classification PE3454336 or ASTM Designation D1248, Type 3, grade 34, Category 5. (9).

TxDOT specifically addresses corrosion in regards to PE duct. They require the material to be non-reactive with concrete, shall not enhance corrosion and be free of water-soluble chlorides.

In addition to composition and corrosion, is the ability of the PE duct to resist pull out. TxDOT requires the duct to show the pull-out force to be equal to 40 percent of the ultimate tensile strength of the bar or tendon that can be transferred from the tendon through the duct to the surrounding concrete at a length of two-feet six-inches.

3.3.5 Galvanized Duct. Galvanized duct provides a rigid duct that can have a greater tolerance toward construction. Earlier research from West and R.P. Vignos of The University of Texas at Austin, indicates that steel duct will corrode across a joint. (23) This emphasizes that a metal duct will not likely provide an effective long term barrier to the tendon. The TxDOT specifications provide little directive in reference to metal duct regarding corrosion. The specifications define the type of steel, American Institute of Steel Construction (AISC) Manual properties, and meet the ASTM requirements of A53, Grade B. (TxDOT Specs.)

The pull-out criteria mentioned above also applies for galvanized metal duct. In addition, the specifications provide for a welded or interlocked seam. The galvanized duct used in the column specimens is a 2-inch galvanized duct with an interlocked seam. The rigid duct was easily installed and provided a firm connection at the dead end of the post-tension as well as the top of the column prior to casting. At the column foundation

interface, inserting the 2-inch steel duct into the hard rubber gasket protected the joint. The AASHTO Specifications mirror the TxDOT specifications regarding metal duct criteria. The requirements are the same. AASHTO requires that the diameter of the duct be ¼-inch larger than the bar diameter. The thesis specimens are in compliance with the above referenced specifications.

3.3.6 Grouts. In the last ten years, grouting has received a large portion of the researchers attention. Grout is the last line of defense for the prevention of corrosion and the influx of chlorides and water. The researchers and their publications are currently ahead of the specifications. These studies have attempted to optimize both grout and material properties and placement techniques. TxDOT Specifications require a Type I or II cement with a maximum water-to-cement ratio of 0.44. An expanding agent is required to provide 2-4% expansion. The expansion agents must not contain any chlorides, fluorides, sulfites, nitrates, aluminum powder or, “ *any other corrosive elements.*” (TxDOT) Fly ash is permitted as a replacement, by weight, of up to 35% of Type A ash. The TxDOT Type A ash is the Class C equivalent. When the fly ash is used, TxDOT permits additional water for workability. The TxDOT Specification Section 426.3 does not place a limit on the additional water. The addition of fly ash should increase the workability without an increase in water.

Project 1405 tested several grouts and additives within the grout through accelerated corrosion tests. The goal of the accelerated testing was to determine the relative effectiveness of various grouts. The author, Mr. Bradley Koester, evaluated several grouts and grout additives. The results of the accelerated grout test revealed surprising results. The maximum TxDOT water/cement ratio of 0.44 was maintained while adding an expansive agent. The time to corrosion was approximately 40% higher than Koester’s base case grout of Portland cement and distilled water. In addition, a comparison of water/cement ratios of 0.44 versus 0.40 was performed. The water/cement ratio of 0.40 had a time to corrosion that was 29% less than the water/cement ratio of 0.44. (Koester)

To evaluate the columns, the research team chose to remain within the TxDOT guidelines using a maximum water/cement ratio of 0.44. This criteria was selected in light of the fact that Project 1405 had already performed a significant amount of grout testing by Mr. Koester and therefore, did not cite the grout as an additional control variable. The research team did elect to use the maximum amount of Class A TxDOT fly ash allowed, 35% replacement by weight.

3.4 Specimen Preparation. To prepare the column specimens, the foundation had to be designed and built first. The design of the foundation had to incorporate two main ideas. First, the foundation had to be able to resist the corrosive elements of the test on the columns. Each of the wet/dry cycles would drain and pond on the foundation. Therefore the concrete had to be a dense matrix of low permeability. In addition, the reinforcement in the foundation could not corrode or the applied service load and moment would be lost. The second consideration was strength. The foundation had to be designed to handle the dead load of the columns, the service load and moment applied to the columns and the P/T force, which is terminated in the foundation.

3.4.1 Foundation Design. To apply a service load and moment to the column specimens a steel load plate would be post-tensioned from the top of the column to the bottom of the foundation. The post-tensioning bars are attached at each of the plate's corners. This allows for eccentricity to be applied to the column and thus, a moment can be applied. Figure 3.5, illustrates the load plate schematic.

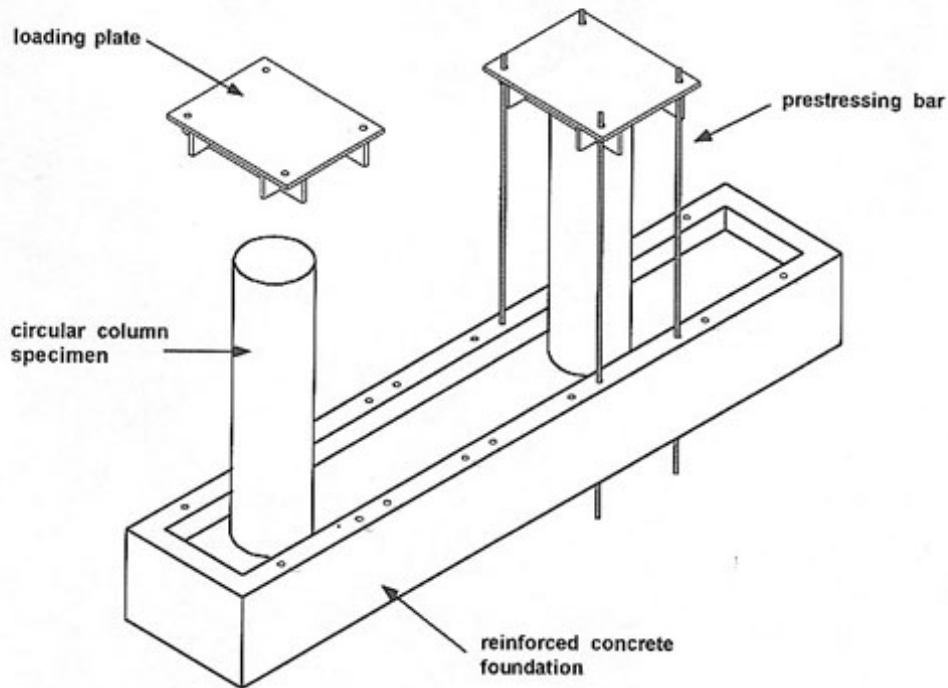


Figure 3.5: Schematic Diagram of Loading Plate and Foundation Detail

The applied service load, from Chapter 3.2.2 is 75 kips, excluding losses. This service load can be applied through four Dywadag bars. The design force in each bar is 35 kips. This force accounts for losses in the bar, moment considerations and seating of the plate. The service load stress in the bars will need to be checked on a quarterly basis to insure that the service load is sustained. As mentioned earlier in Section 3.2.2, the Service moment applied is 225 kip-inches. The applied Service load is 75 kips and the distance from the center of the column and/or load plate to the center of the applied force

is 13.5 inches or e_{bar} . The applied load at each bar can be calculated from Equation 3-7, below.

$$P_1 = 0.5[P_{\text{service}} + M_{\text{service}}/ e_{\text{bar}}] \quad (3-7)$$

Given as stated above that P_{service} is equal to 75 kips and M_{service} is equal to 225 kip-inches, then P_1 is equal to 45.8 kips. In addition, the service load P_{service} is equal to:

$$P_{\text{service}} = P_1 + P_2 \quad (3-8)$$

Therefore P_2 is equal to 29.2 kips. To design the foundation system, the design force in each bar was assumed to be 35 kips. The foundation would have to resist the four service load bars equaling 35 kips each, plus the force of the P/T bars. The strut and tie method was chosen to design the foundation to resist the applied axial force. This method is well suited for the design of deep footings, pile caps, and pier caps. Some of the specimens modeled the TxDOT column pier cap interface. Therefore, this method appears to be a logical choice.

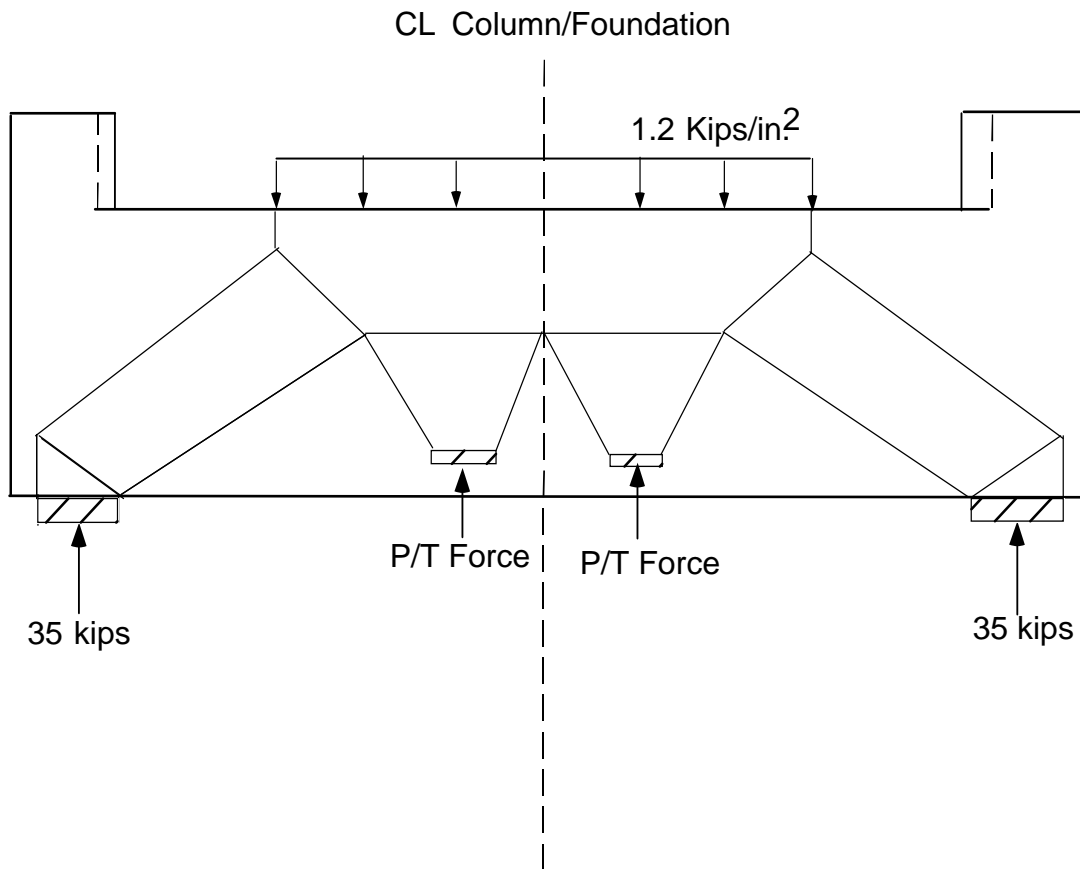


Figure 3.6: A Schematic Strut & Tie Model for the Foundation Under a Typical P/T Column

The compression fan is generated from the external force applied through the four Dywadag bars. A large plate at the top of the column specimen transfers this load onto the specimen. At the bottom of the column specimen there is a large compression node. This node receives the force of the service load on the column specimen, the dead load of the member and the P/T force. The forces in the strut and the model depicted above can be determined from basic geometry. Consider the reaction at the nodes below the service load bars at the bottom of the foundation. The service load creates a compression fan force in C_1 from the schematic above of 68.3 kips. These forces, as

well as the rest of the members, are determined from the geometry. The rest of the forces are:

$$T_1 = C_2 = 36.10 \text{ kips}$$

$$C_3 = T_2 = 30.94 \text{ kips}$$

In addition to the geometry of a typical section is the calculation of the nodes. In determining the stress, several design assumptions were made. They are:

- The 28-day compressive strength of the concrete, f'_c , is 8,000 psi.
- The design of the foundation is based on the 1994 AASHTO Specification.
- The nodes at the loading points remain the same.

In order to distribute the compressive stresses equally under the column, the research team elected to rotate the P/T bars. Figure 3.7 illustrates, in plan view, the orientation of the P/T bars in relation to the compression struts as a result of the service loading. To determine the limiting compressive stress, f_{cu} , the 1994 LRFD provides the following equation:

$$f_{cu} = \frac{f'_c}{0.8 + 170\varepsilon_1} \leq 0.85f'_c \quad (3-8)$$

Where f'_c is the 28 day compressive strength of the member, ε_1 is defined in the AASHTO LRFD Equation 5.6.3.3.3-2 as:

$$\varepsilon_1 = (\varepsilon_1 + 0.002) \cot^2 a_s \quad (3-10)$$

The variables in equation 3-9 above are defined by AASHTO as:

- ϵ_s is the tensile strain in the concrete in the direction of the tension tie in in./in.
- a_s is the smallest angle between the compressive strut and the tension ties in degrees.

If the concrete is not subjected to principal tensile strains greater than 0.002, then the concrete can resist a compressive stress that is equivalent to approximately 0.85 f'_c . As the reinforcement of the tension ties approach yield in tension, there will be increased tensile strains imposed on the concrete. As these strains increase, the compressive stress, f_{cu} , decreases. In addition, if the angle decreases, ϵ_1 increases and the compressive stress decreases. Hence, if the angle, a_s , approaches zero, no compressive stresses would be allowed in the compressive fan. If the strain of the tension reinforcement varies over the width of the strut, the code allows the centerline value of the strain, ϵ_s , to be used.

(10)

The stress from T_1 , ϵ_s , based on the code discussion above is calculated to be 0.00156 in./in. Therefore the compressive stress from Equation 3-8 is determined to be 4.77 ksi. Finally the strength of the compressive strut can be determined from the area of the strut, A_c , which is determined from the geometry of the member to be 24.5 in². The AASHTO code has a resistance factor, ϕ , of 0.7 for strut and tie analysis. Considering the area and the resistance factor, the actual design strength in the compressive strut is determined by Equation 3-11 as:

$$P_u = \phi A_c f_{cu} \quad (3-11)$$

Where P_u is the allowable force in the compressive strut. The value is determined to be 81.7 kips for the foundation member. This force exceeds the applied compressive forces in C_2 and C_3 .

In order to design the tension forces, 4-#4 bars are selected. This will carry the tension ties, and the foundation stirrups are selected as #4 ties at 6-inches on center. This

area of steel, 0.8 in.^2 will provide a tension force equal to 43 kips which is greater than the required force, T_1 or T_2 . A similar analysis is performed for the compression force induced from the Post-Tensioning force. As expected, the previous values are more conservative and will be used.

The issue of the center node underneath the column had to be analyzed so that bursting stress was taken into account. The bursting stress, or stress resulting from the bursting force, will have to be calculated next. AASHTO defines the bursting force as the tensile force in the anchorage zone acting ahead of the tendon device and transverse to the tendon axis. The bursting force, T_{burst} , is defined by the AASHTO Equation 5.10.9.6.3-1. The bursting force in the foundation determined from this equation is 25-kips. The reinforcing confinement required is two #4 stirrups transverse to the tension area or general zone.

To determine the area to be considered for bursting stresses, the AASHTO Code considers two zones, the local zone and the general zone. AASHTO defined the local zone as “*the region of high compression stresses immediately ahead of the anchorage device.*” The criteria that must be met for the local zone are dependent on the transverse direction. The Code states that the dimensions of the local zone in each transverse direction shall be the greater of:

- *the corresponding bearing plate size, plus twice the minimum concrete cover required for a particular application and environment and,*
- *the outer dimension of any required confining reinforcement, plus the required concrete cover over the confining reinforcing steel for the particular application and environment.*

The critical component in relieving the stresses under the column to allow the node to receive all of the compressive struts was to rotate the P/T bars 90° as shown in

Figure 3.7. This prevents an overlap into the node under the column from any one strut. The dead end anchorage, a 3-inch x 3-inch plate has a resistance force of 48.2 kips. This force, of 48 kips, is greater than the applied force with a 1.4 increase of 37 kips. The bearing capacity was determined from the AASHTO Code Equation (5.10.9.7.2-1). The area of each of the dead end anchorage plates defines the local zones and confirms that no additional confinement is required in the local zone.

A significant component of the general zone is the area ahead of the anchorage. AASHTO limits the amount of stress in this area in Section 5.10.9.4.3. The requirement is that the stress ahead of the anchorage device shall exceed the Code Equation, 5.10.9.6.2-1. The concrete stress in the foundation ahead of the P/T anchorage is required from this equation to be 2.36 ksi. The concrete compressive stresses provided in the foundation are 3.92 ksi. Thus, the area ahead of the anchorage is controlled by the 8-ksi concrete strength provided. Detailing of the additional confinement required in the general zone is defined in Section 3.4.2

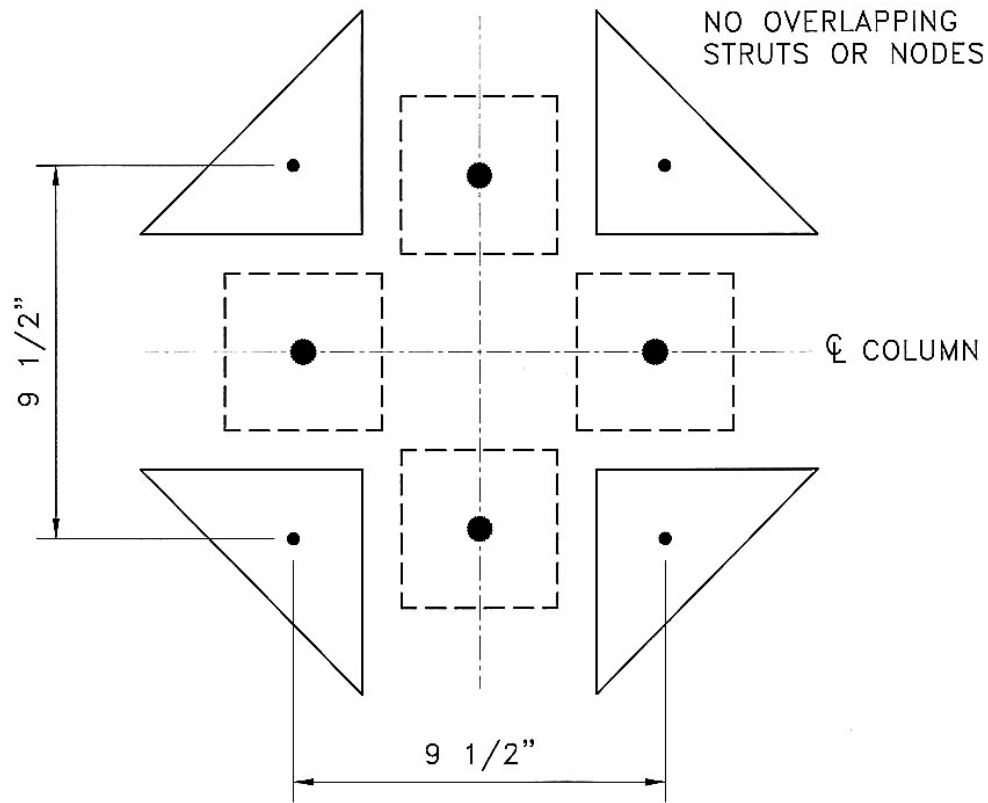


Figure 3.7: Plan View of Compression Struts after the 45° Rotation

3.4.2 Foundation Reinforcement. The foundation was cast in the Ferguson Structural Engineering Laboratory and moved outside with a forklift. The foundation rests on three 10-inch supports on top of a bed of gravel. The reinforcement for moment and shear was determined from conventional analysis. The reinforcement provided in the bottom is #6 bars, as shown in Figure 3.8. The ties are determined from standard ACI Design criteria. In addition to the stirrups required for shear reinforcement are the additional stirrups provided as tension ties determined in the design section above.

Finally, horizontal reinforcement to control bursting in the general zone is provided by 3-#4 bars on 6-inch centers below each of the columns.

Once the detailing issues were completed for the foundation the corrosion protection design needed to be completed. Epoxy bars were chosen for the protection scheme as well as epoxy ties. Care had to be taken to prevent contact of the terminal end section of the P/T bars to ensure they did not come into contact with the epoxy reinforcement. All of the bursting reinforcement that surrounded the terminal ends of the P/T bars were also epoxy-coated reinforcement. Care was taken at the raised sections to insure that there was zero cracking at the bottom of the wall-trough interface.

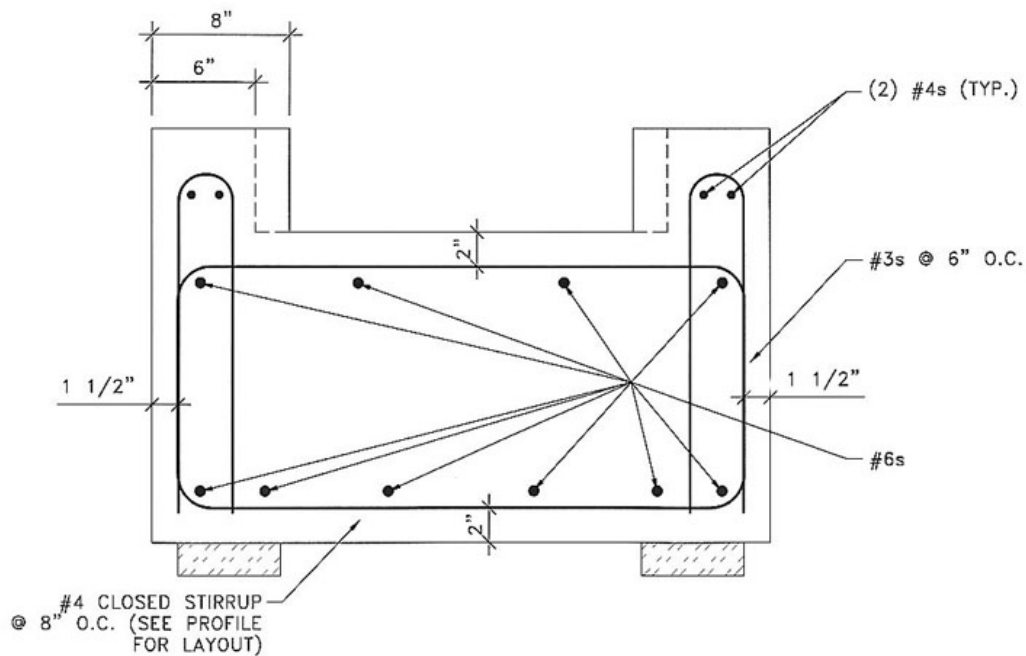


Figure 3.8: Column Foundation Section

3.4.3 Foundation and Column Formwork. Upon completion of the design of the

reinforcement, the reinforcement cage was built on top of a false plywood deck. Epoxy coated slab bolsters were provided to insure clear cover on the bottom of the foundation. Figure 3.9, displays the reinforcement cage prior to completing the formwork.



Figure 3.9: The Foundation Reinforcement Prior to Forming

The outside form walls were constructed of $\frac{3}{4}$ -inch plywood and conventional 2 x 4 framing with studs on 16-inch centers. Once the perimeter of the foundation form was completed, the depressed section, which serves as the trough, was built next. To provide for the deepened section, 2 x 8's were beveled on one side at a 45° angle. The curb width was held to 8-inches. This distance did not provide enough clearance between the

column and the curb wall. At the column sections, the curb width was designed and built to be 6-inches. Styrofoam blocked out the areas where a 6-inch curb was required. Figure 3.10, depicts the curb layout in plan view. The holes shown in Figure 3.10 are designed so the service load stressing bars can pass through the foundation.

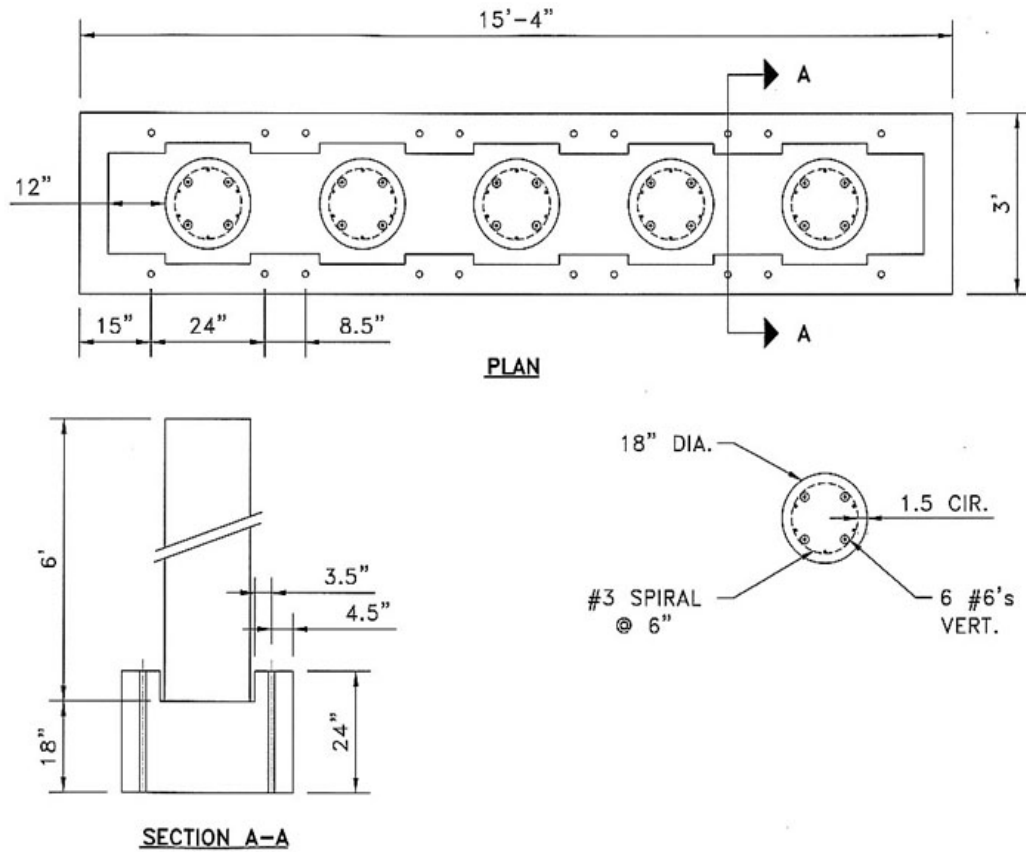


Figure 3.10: Schematic of Holes for Service Load P/T Bars

In order to ensure that corrosion does not occur at the foundation curb, 2-inches

of cover is provided around the bar ‘ *sleeves*’. To form the sleeves, 2-inch polyvinyl chloride (PVC) pipe is cut in 24-inch sections.

To insure that the pipe sleeves would not move, 1-5/8-inch plugs are cut from plywood and nailed to the bottom of the form at the sleeve’s exact location. The tops of the sleeves are capped so no concrete can enter the tubes. Figure 3:11 displays the pipe sleeves.



Figure 3.11: The Pipe Sleeves for the Service Load Post-Tensioning Bars Prior to Casting

Casting for the foundations occurred inside the Ferguson Laboratory. The foundations were cast by means of a $\frac{3}{4}$ yard bucket. The concrete slump was typically measured between 3-4 inches. The concrete was properly consolidated with two (2) 1-1/2-inch vibrators. The entrained air was within the mix design acceptable limits. The mix design chosen for the foundation members was Capitol Aggregate Mix # 221 and #

224. Both of these mixes used a high strength aggregate; ½- inch Burnet course aggregate. In addition, 35% fly ash by volume was used to enhance the impermeability of the foundation concrete. The 28-day strength break on the concrete used in foundation #1 was recorded at 8,480 psi. This strength was well beyond the design requirement of 5,000 psi. No deficiencies were noted for this pour.

The second foundation was cast in the laboratory on March 28, 1996. The mix design was improved to use a more workable mix design. In order to maintain the high strength property while increasing the workability, the mix design for the second pour was changed. The revised mix design was Capitol Aggregate Mix # 226. The mix design, for a 3.5-yard batch, consisted of the following proportions:

Sand	5068	lbs.,
1/2" Rock	5827	lbs.
Cement II	2499	lbs.
Fly Ash	889	lbs.
Water	251	lbs.
Rheobuild	560	oz.
Air	0	oz

The Rheobuild is a High Range Water Reducer (HRWR) or superplasticizer. Since the foundation concrete is not in any way a test specimen, the research team elected to use the Rheobuild Product to lower the required water, thus increasing the impermeability of the foundation concrete. No problems were noted for the second foundation pour. The strength results were very favorable for the second foundation. Eight cylinders were cast for strength evaluation of the second foundation. The average strength breaks based on two cylinders per test are as follows:

- 7-day 5,100 psi.

- 14-day 7,540 psi.
- 28-day 8,480 psi.

After casting, the foundations were cured with wet burlap for seven days in the laboratory. The burlap was dampened periodically to ensure the burlap remained damp. Upon completion of the curing of the foundations, the concrete was “rubbed out” to seal all form marks and voids. This rubbing was completed as a typical TxDOT substructural component as an “Ordinary Finish” with latex grout filling in the voids.

Upon completion of the foundation surface preparation, the column formwork could proceed. The first five column specimens prepared were Column Specimen Numbers 1,3,4, 6, and 8. These columns do not have post-tensioning in the specimens. The reinforcement cages are tied on the ground and stood up on the foundations. Once the reinforcement cages were in place, the half-cell wiring was installed. Two No. 8 gage, red coated wires were clamped directly to the #-6 vertical bar approximately 12-inches from the bottom and 6 inches from the top of the specimen. Cardboard sono-tube was used as the exterior form. Wood bracing was installed at the bottom and top of the form. Wood screws mounted the bracing on top to the sono-tube forms. Figure 3.12 displays the completed column forms on Foundation 1.



Figure 3.12: The Completed Column Specimen Forms on Foundation 1

The first foundation cast was forklifted to the final testing area behind the Materials Building where a level pad was constructed on 4 x 6-inch timbers to support the foundations.

3.4.4 Epoxy Connections. A critical aspect of the post-tensioned columns is the interface at the foundation. As mentioned in Section 3.2 of this thesis, hard rubber gaskets are used to depress the duct into the foundation. Gum rubber with a mild hardness was selected. In addition to the gaskets, the duct for the P/T bars must contain a grout tube at the bottom of the duct to inject the grout into the duct. Figure 3.13 displays the duct inserted into the gasket with the grout tubes inserted into the duct.

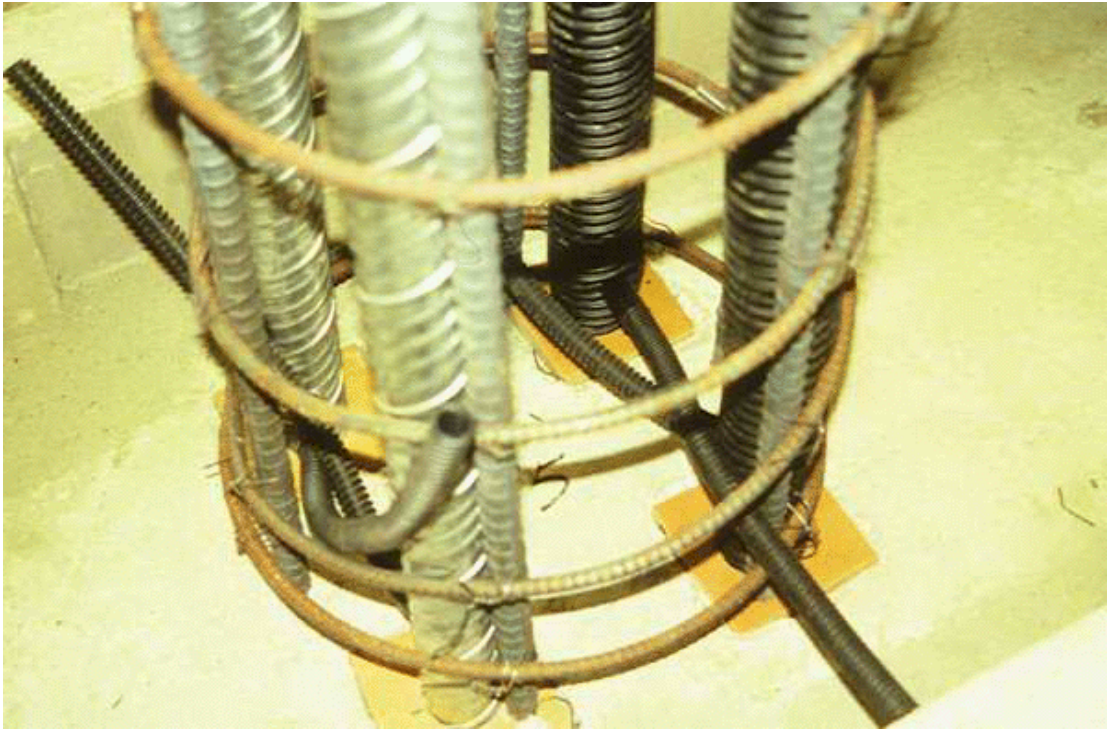


Figure 3.13: The Bottom of the Column Cage Illustrating the Duct

3.4.5 Concrete Casting. Once in place, behind the Materials Laboratory, the columns were braced down to the ground to ensure the column specimens were plumb. Using a $\frac{3}{4}$ -yard bucket with a five-foot tremie to eliminate segregation in the concrete, the concrete casting was completed. The University of Texas forklift was employed to hoist the bucket. Figure 3.14 illustrates the casting operation.



Figure 3.14: Casting Columns on Foundation 2

The casting for the Class C concrete column specimens 1, 3, 4 and 6 on Foundation 1 were completed on January 25, 1996. The air temperature was 71° and the weather was sunny and clear. Plastic was used as a means to protect the concrete

specimens after casting. The evening temperature low was 47°. Two concrete tests were run to be consistent with TxDOT Specifications. The slump was measured at 3.5 inches. Column Specimen 8 was cast on February 25, 1996. Once again the weather was favorable for casting. The air temperature was 67° with a slight overcast sky. As before the same concrete protection scheme was used with plastic sheets. All of the concrete cylinders were cast adjacent to the specimens and cured in the exact same manner. Table 3.5 below lists the concrete compressive strength values, measured in pounds per square inch, for Column Specimens 1, 3, 4, 6, and 8.

Table 3.5: Compressive Strength values for Columns 1, 3, 4, 6 & 8

Column	7-Day Strength (avg.)	14-Day Strength (avg.)	28-Day Strength (avg.)
1	4,790 psi.	6,175 psi.	6,090 psi.
3	4,790 psi.	6,175 psi.	6,090 psi.
4	4,790 psi.	6,175 psi.	6,090 psi.
6	4,790 psi.	6,175 psi.	6,090 psi.
8	3,788 psi.	5,776 psi.	6,240 psi.

As with many tests there are many variables with concrete compressive strength tests. Variables include different test operators, precise loading of the specimens in the test apparatus, transportation of the cylinders, and casting of the molds. Significant in Table 3.5 is the decrease in strength between the 28-day and 14-day tests. Based on experience, a decrease in strength seems highly unlikely. The decrease in these results is attributed to a flawed test. Several people performed these tests from casting to the actual breaking and recording. Therefore, the possibility of an error seems likely. Two more cylinders were tested at 56-days. The compressive strength results at 56-days are an average of 6,735 psi. These results assure that the strength results for these first four column specimens are adequate. That was noted in the first strength tests and the

researchers attempted to reduce the number of people involved. The compressive testing variability improved after these results.

Upon completion of Foundation 2 the same forming procedure was used to prepare the second set of column specimens for casting. The second set of columns were placed 10 feet North of Foundation 1 on the same pad. Both foundations then can be serviced from the same irrigation system. The irrigation system will be presented and discussed in Section 3.5.2.

The casting for Columns 2, 5, 9 and 10 was completed on April 18, 1996. The temperature was warm and the weather was windy. The slump of the concrete was measured at 4 inches. The concrete pour went well and no problems or deficiencies were noted. Column 7, which contains 35% Fly Ash was the last column to be cast. The column was cast on April 29, 1996. Again the weather was fair but windy. The air temperature was 82°. The pour was completed in a short time. Several cylinders were taken and no deficiencies were noted. Table 3.5 displays the concrete compressive strength values for the columns 2, 5, 7, 9, and 10.

Table 3.6: Compressive Strength values for Columns 2, 5, 7, 9 & 10

Column	7-Day Strength (avg.)	14-Day Strength (avg.)	28-Day Strength (avg.)
2	3,925 psi.	4,325 psi.	4,480 psi.
5	3,925 psi.	4,325 psi.	4,480 psi.
9	3,925 psi.	4,325 psi.	4,480 psi.
10	3,925 psi.	4,325 psi.	4,480 psi.
7	5,107 psi.	6,028 psi.	6,706 psi.

After casting the second set of columns for Foundation 2, a closure pour needed to be completed. The closure pour encapsulated the top of the four post-tensioning bars. The column caps, on Column Specimens 2, 5, 7, 9, and 10, were approximately 8-inches in height. The caps were poured after the completion of the post-tensioning. To

complete this section of the columns, the research team mixed their own Class C concrete from the materials at the University of Texas’s materials laboratory. Table 3.7 provides the mix design for the column closure pours with fly ash. The compressive strengths from this mix were as follows:

- 7-day 5,090 psi.
- 28-day 6,180 psi.
- 56-day 6,780 psi.

The use of fly ash in the closure pour was chosen to increase the strength.

Table 3.7: The Concrete Batch Design for Concrete Closure Casting

Mix	RGC1
Coarse Aggregate	1838 lbs.
Aggregate Type	½” River Gravel
Water	250 lbs./cy
Cement	658 lbs.
Cement Type	Capitol I/II
Fine Aggregate	1294 lbs.
Recommended Slump	3”
Retarder	3 oz.

The column caps were cast on 5-12-96. The cement used in the laboratory was all labeled Type I/II in 55-gallon drums. The cement, as shown above, was a Type I Capitol cement. During the grouting of the P/T ducts, all the remaining cement in the existing 55-gallon drum was exhausted. A second drum labeled I/II was used for the caps. The drum turned out to be mislabeled. Upon removal of the cap forms, the concrete spalled away easily. A bare hand could remove portions of the column caps. The team learned that what they thought was Type I cement in the second drum was

actually Class F fly ash.

The column closure pours were removed and recast on May 21, 1996 with the proper cement in the mix design. The error was of no consequence to the column closure pours. However, it was possible that one or two tendons could have been affected by a combination of cement and Class F fly ash at the end of the grouting stage. Further testing by the research team at a later stage may be required to verify Type I cement in the entire duct.

3.4.6 Post-Tension Stressing / Grouting. The column specimens on the second foundation were allowed to cure for a minimum of seven days prior to stressing. The compressive strength target was 4,000 psi. Each of the columns exceeded this benchmark. A single ram was used to pull each bar. In order to determine the amount of stress and ultimately the amount of force in each bar, a load cell was used. The load cell was placed between the ram and the jack stand. The load cell was calibrated to the following:

$$1 \text{ kip} = 0.201\text{mV} \quad (3-12)$$

Based on this relationship, the bars were stressed in 10-kip increments rotating clockwise around the column. Table 3.8 gives the following post-tension values for each of the columns.

Table 3.8: Field Calculations for the P/T Stressing of the Columns

Column No.	Bar	Voltmeter Reading(V)	Applied Force (kips)
2	NE	0.006193	32.4
	NW	0.006193	32.4
	SE	0.006212	32.4
	SW	0.006210	32.4
5	NE	0.006190	32.5
	NW	0.001695	32.4
	SE	0.006192	32.4
	SW	0.006193	32.4
7	NW	0.006212	32.4
	NE	0.006197	32.4
	SE	0.006191	32.4
	SW	0.006213	32.4
9	NW	0.006192	32.4
	NE	0.006201	32.4
	SE	0.006193	32.4
	SW	0.006202	32.4
10	NW	0.006175	32.6
	NE	0.006183	32.3

The additional force of approximately 2.4 kips was determined from trial and error to be the correct force to compensate for seating losses. Figure 3.15 illustrates the post-tensioning of the P/T bars in the column.



Figure 3.15: Stressing of Column 5 P/T Bars

The Post-tensioning of the columns was completed with only one incident. On Column Specimen 5, local crushing of the concrete occurred at one corner of the plate washer on top of the column on the Northwest bar. Dr. Breen and Dr. Kreger investigated the damage and determined that the crushing was localized and incidental to the column. No significant losses were attributed to this condition.

In order to complete the post-tensioning, the grouting of tendons was the last order of business. Compared to the prototype column, the model was not only small in diameter but very short as well. Typically, the post-tensioning system would have a vent tube at the top of the duct. Due to the size of the column the vent tube was eliminated. To accomplish venting at the top of the duct, two (2) 3/16-inch holes were drilled through the washer into the duct below. The grout was then injected from the tube located at the base of the column and forced out the small holes in the washer on top of the column. Once the grout streamed out of the small holes in the washer, the holes were

plugged with small screws.

The typical duct used approximately 0.8 gallons of grout for the plastic duct and approximately 0.5 gallons for the galvanized duct. The material was carefully measured to maintain the specified water-to-cement ratio of 0.44. Once the cement and the water were weighed and mixed, the grout was injected into the grout tubes at the bottom of the column and pumped out through the small holes in the washer at the top of the column. This procedure was repeated for all 20 ducts over two days. Upon completion of the grouting, the specimens were prepared for the closure pours discussed earlier on page 90. The excess tendon length was cold cut with a hacksaw to ensure that the tendon was not affected by heat. The cover provided from the post-tension anchorage to the top of the closure pour exceeded 3 inches in length.

3.5 Test Setup. In order to match the 3/5 scale column with the prototype TxDOT Bridge column, the loading and the column's exposure environment must be reproduced at the laboratory. This section will explain in detail how the experiment duplicates these conditions of service loading and exposure.

The force required to simulate the loading condition will be transmitted through the foundation. All of the steel components used to simulate the service load will be sand blasted to bare white metal and painted with an epoxy paint system. This special paint system will ensure that the loading components were not affected by the exposure conditions that the column specimens will be subjected to. Each component of the test, excluding the columns themselves, had to be designed to resist the corrosive environment the columns would be subjected to.

3.5.1 Service Load Application. The final step in the specimen preparation was to apply the service load and moment. As discussed in Section 3.2.2, the amount of moment was equal to M_{service} . The amount of service moment, M_{service} , is 225 kip-inches. The applied service load, P_{service} , is 75 kips. This service load had to be applied to 8 of

the 10 columns under service load. The columns to which the service load is applied are listed in Table 3.9 below.

Table 3.9: The Column Specimens under Service Load

Specimen Number	Concrete	Foundation Connection	Applied Axial Load	Applied Moment	Comments
1	Class C	TxDOT Doweled	0	0	Unloaded
2	Class C	Post Tension	0	0	Unloaded
3	Class C	No Joint	0	0	Unloaded
4	Class C	TxDOT Doweled	75 kips	225 k-in.	Service Load
5	Class C	Post Tension	75 kips	225 k-in.	Black P/T Bar
6	Class C	No Joint	75 kips	225 k-in.	Service Load
7	35% Fly	Post Tension	75 kips	225 k-in.	Low Permeability
8	Ash 35 % Fly Ash	TxDOT Doweled	75 kips	225 k-in.	Low Permeability
9	Class C	Post Tension	75 kips	225 k-in.	Epoxy P/T Bar
10	Class C	Post Tension	75 kips	225 k-in.	Galvanized P/T Bar

In order to apply both the moment and the service load to the columns, the foundation, as mentioned in the foundation section, was used to anchor four 1-1/4-inch Dywadag bars. The four bars run through the plastic sleeve in the foundation to a 4-inch square plate washer 3/4-inch in thickness. These four bars run through a large 1-inch steel plate which sits on top of the column. The plate is designed to resist the moment due to the applied force at each corner of the plate. To provide stiffness to the plate and to insure that the plate fits snug on top of the column, 6-inch by 1-inch stiffeners were used. The stiffeners deepen the centroid of the section. The plastic moment of the section, M_p , is calculated to be approximately 1,350 k-inches. The applied moment on the steel plate in the long direction, parallel to the foundation, is approximately 500 kip-inches. Therefore, the plate was able to resist the applied moment. The shear strength of

the plate was also verified. The weld strength is 22.6 kips per inch.

In order to apply the service load, a loading plan was in order. Two of the bars would be jacked to a force of 45 kips and two bars would be jacked to 30 kips. This difference in force in the service load bars applies the moment to the column. To advance the force in all of the bars simultaneously, two jacks will be employed to stress the four bars. Because the applied force is greater in two of the four bars, a beam will be used to transmit the force from the jacks to the bar. Two C-Channels were placed back to back with a 1-1/2- inch space between them. Flat plate washers were welded at the top where the bar penetrates the C-Channel and at the bottom of the two C-Channels to receive the jack piston.

The C-Channels were designed to resist moment stresses, shear stress as well as web yielding and web crippling. Based on these criteria, 2 C8 x 11.75 members were chosen. As with the plates the C-channel design was based on the AISC steel design code 1994 edition. Figure 3.16 illustrates the jacking procedure with both C-channels and jacks in place.



Figure 3.16: Service Load being Applied to a Column Specimen

The application of the service load was very similar to the post-tensioning of the columns. In the service load case, two load cells were sandwiched between the 1-inch service load plate and the ram as shown in Figure 3.16. Notice in Figure 3.16 that the hydraulic rams were inverted to insure that the cylinder of the ram was directly in the center of the load cell. The ram model employed was a model No. RC 613T. To insure accurate readings from the load cells, pressure gages were attached to each ram to measure the applied force by gage pressure. The surface area of the ram is 13.75 square inches. The applied force required for the bars are 45,000 lbs. and 30,000 lbs. Therefore the gage pressure is determined by dividing the area into the applied force. The two gage pressures, when the service load is applied, should read 3,273 psi. for the 45 kip force and 2,182 psi. for the 30 kip force.

As before, a voltmeter was wired to the load cell to determine the jacking force. Figure 3.17 illustrates the simple wiring schematic from the load cell to the digital

voltmeter.

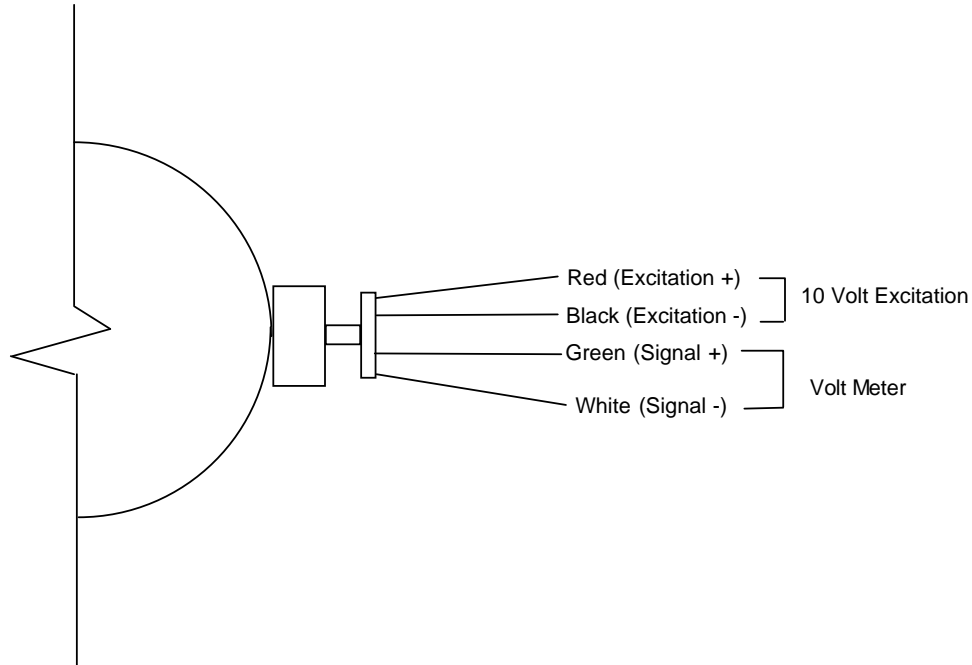


Figure 3.17: Wiring Schematic of the Load Cell to the Voltmeter

In order to jack the bars evenly, the initial columns, 1 and 2, were jacked in increments of 3.33 kips for the 30 kip bars and 5 kips for the 45 kip bars. The jacking operation would be completed in 9 lifts. The load cells were calibrated to the following:

- 100 kips = 20.1 mV (for the 30 kip bars)
- 100 kips = 30.1 mV (for the 45 kip bars)

As with the post-tensioning of the columns, the anchorage losses were of a concern to the research team. The Dywadag nuts, which hold the bar in place, were tightened at the end of each lift increment. A 6-foot pipe extension on the end of a box wrench was used to tighten the nuts once the final jacking force is applied. The jacking force was released and then reapplied to ensure that the final position force was exceeded

before the nut was loosened. This anchorage check was completed and assured the researchers that the applied force was sustained.

3.5.2 Irrigation System. The exposure condition for the columns needed to duplicate actual events that are occurring in the TxDOT bridge columns. The geographic regions had differing exposure conditions that must be considered. The research team chose two very important conditions that are prevalent in the entire state in some fashion. One is the wetting and drying cycle. The wetting and drying cycle will be employed on one half of each column specimen.

The second condition is the ability of the exposure testing, to recreate the possibility of wicking above the water level. This phenomenon presents the problem of sustaining a water table of salt water. As discussed earlier, this will be accomplished with a trough in the foundation. The foundation itself cannot corrode or the post-tensioning and/or service loads could be compromised. Every effort was made to protect the foundation. These steps included low-permeability concrete, epoxy-coated reinforcement, plastic for all components of the foundation exposed to the environment and the pool paint coating for the inside of the foundation exposed to the ponded water.

The salt water is pumped from the foundation to a reservoir. This reservoir in turn feeds a system of plastic irrigation pipes on top of the column specimens. Each column has a grid mapped on the column to identify the exact location of reading to monitor corrosion. The amount of salt, in the form of NaCl, is chosen to be 3.5 %. This is a fair duplication of seawater. However, this amount of salt may not represent the amount of salt from de-icing salts applied to bridge decks.

In addition to the salt from de-icing operations are new brands of anti-icing and de-icing chemicals. These chemicals include magnesium chloride, calcium magnesium acetate, and calcium chloride. The affect of these anti-icing and de-icing chemicals on Texas Bridges, also needs to be determined. Early evidence suggests that magnesium chloride may be more corrosive than NaCl. (22). This chemical is used in the upper Midwest and northeast. The chemicals low eutectic temperature allows magnesium

chloride to melt ice at a very low air temperature. Common road salts, used today, cannot duplicate this feat. Magnesium Chloride used in de-icing and anti-icing is coupled with a corrosion inhibitor. These inhibitors are generally a form of a zinc molecule, which are substantially larger than the chloride ion. The corrosion inhibitor is added to prevent flat metal corrosion, in other words, corrosion of automobile components. Little research has examined the effect on bridges. These “new” breeds of chemicals will need to be researched in the future to study their affect on concrete reinforcement. The amount of salt water applied to the columns and the duration of the application will be addressed in future research conducted by the University of Texas. This portion of the project was beyond the scope of this thesis.

The apparatus included a stainless steel pump to recycle the water, a plastic reservoir to hold the salt-water solution and a regular garden hose to transport the water from the reservoir to the plastic irrigation pipes. To minimize the amount of evaporation from the foundation, plywood covers cut to the column's circumference were designed to enclose the foundation from above. Figure 3.18 illustrates the complete irrigation assembly.



Figure 3.18: The Column Irrigation System

In addition to Figure 3.18, Figure 3.19 displays a close-up of the irrigation pipes,

which terminate at the top of the column. Along with the irrigation termination ends, Figure 3.19 also shows the black column gridlines.



Figure 3.19: Irrigation Termination Ends and Column Gridlines

3.6 Test Procedure. In order to measure the onset of corrosion in the columns, a series of half-cell readings were used. Earlier, as mentioned in Section 3.4.3., 8 gage wires were installed to measure the voltage potential at each location along the column. In order to record the location on each column, the columns have a unique identification code. The code schematic for each column is displayed in Figure 3.20:

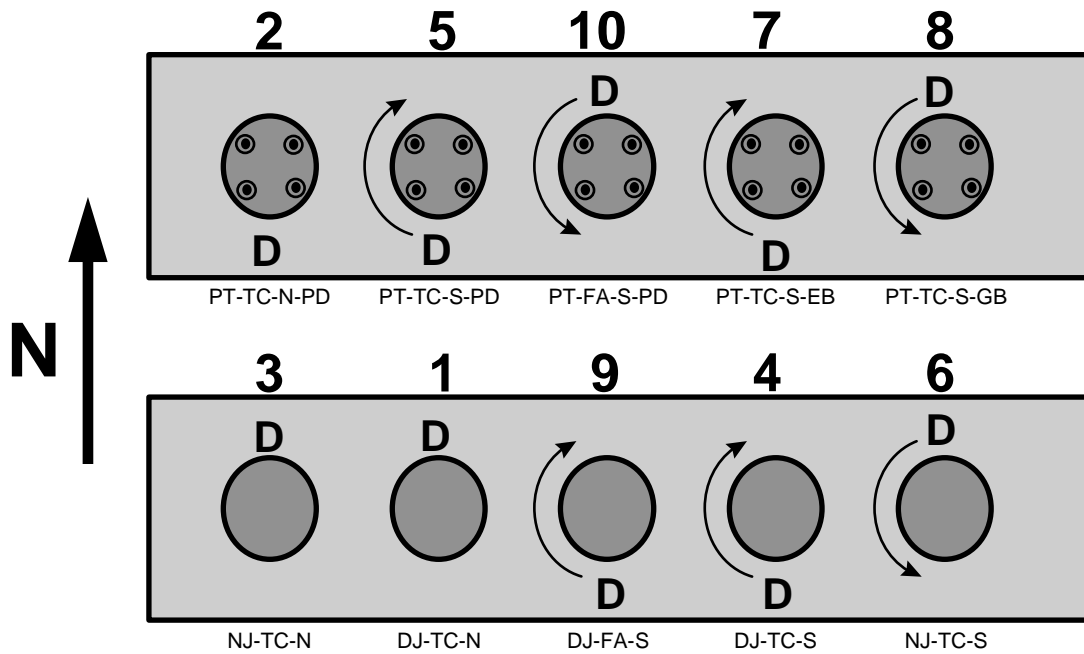


Figure 3.20: Individual Column Designations

In Figure 3.21, the column specimen notation is displayed. This notation will be used in all of the column data description. In addition to the five levels shown, each of the columns have vertical lines going up the column to complete a grid on the column used for half-cell mapping.

PT-TC-S-PD

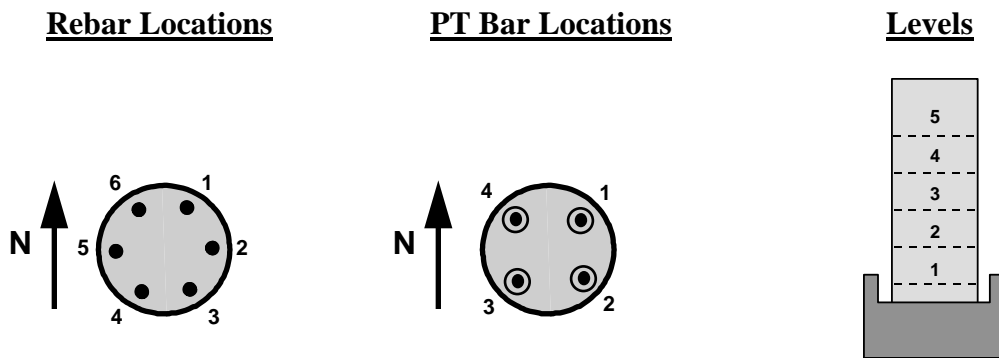
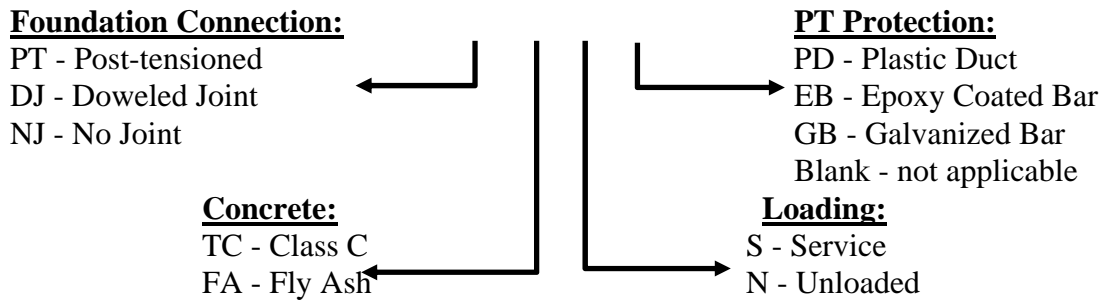


Figure 3.21: Long Term Column Exposure Tests Specimen Notation

3.6.1. Half-cell Potential Measurements. The rate of corrosion, as described in Section 1.3.2 of this thesis, is measured as the Voltage potential between the reference electrode, the saturated calomel electrode (SCE), and the iron half-cell electrode in concrete. The half-cell potential survey is conducted in accordance with ASTM C876, “Standard Test Method for Half-Cell Potentials of Uncoated Reinforcing Steel in Concrete (ASTM), except that the SCE is used in lieu of the sulfate copper/copper electrode (SCE). The SCE is more commonly used in laboratory work. The offset potential for the difference between SCE and CSE is 77mV. A more common amount of 70 mV is commonly used to adjust the ASTM C876 limits. Using the voltage reading of the potential, there is a direct indication of a concentration of Fe^{2+} ions in the concrete surrounding the embedded steel. Typically, the voltage meter is connected to the

electrodes such that the values are normally negative. This is the standard convention for half-cell readings. The range of potential presented will be in three categories. They are:

- more positive than -130 mV SCE, there is less than a 10% probability of corrosion occurring;
- between -130 mV and -280 mV SCE, there is an uncertain probability of corrosion occurring;
- more negative than -280 mV SCE, there is a 90% probability of corrosion occurring.

The differences in voltage as mentioned above, are attributed to the fact that the concentration of ions from the reference electrode remains constant while the Fe^{2+} ions differ. This measurement and subsequent concentration levels of ions is an instantaneous indication of the probability of corrosion activity.

Some researchers have suggested that the ranges of half-cell potential are not accurate. (Elsenor & Bohni) Admittedly, the half-cell test does not provide a rate of corrosion, but the test identifies that corrosion is occurring. The rate of corrosion, and one of its measures, linear polarization, was discussed earlier in Chapter 1. This method could be employed to attempt to measure the rate of corrosion in the specimens. At the time of this thesis, no plans for linear polarization testing have been made for the column specimens. However, the existing pre-wire in the column specimens could be used for linear polarization measurements. In this event several other factors would need to be considered to substantiate the validity of such a test.

3.6.2 Chloride Powder Measurements. The column specimens will absorb some amount of chloride ions through the surface of the concrete due to repeated exposure of salt water. The amount of chloride migration into the concrete matrix of the column

specimen, and eventually to the reinforcing, needs to be closely monitored and documented. The method chosen to document and monitor the chloride progress into the specimens is chloride powder sampling. The sampling will be conducted in accordance with TxDOT's test method, Tex-617-J.

The procedure for chloride analysis, in accordance with the TxDOT Method referenced above, is given in the next four tables, Tables 3.10 through 3.14 and associated text. The complete test is given in Appendix A.

Table 3.10: Procedure for Chloride Analysis

Step	Action
1	Invert and shake the flask well to insure thorough mixing of the solution.
2	Transfer 50 ± 5 ml (1.7 ± 0.15 oz.) of solution to a clean, dry electrolytic tall form beaker with magnetic stirring bar.
3	Add three or four drops of methyl red indicator solution and acidify with the nitric acid solution to a pale pink endpoint while the stirring bar is rotating.
4	Fill the reference electrode chamber with the appropriate filling solutions if the solution levels are low.
5	Rinse and towel dry the electrode surfaces and immerse the electrodes in the sample solution.
6	Turn on the ion meter and place controls in the millivolt (MV) readout setting.
7	Allow the millivolt reading to stabilize by coming to a constant value or a net change of 0.1 MV in no less than five seconds.
8	Record the millivolt reading.
9	Repeat this procedure for each sample solution to be analyzed.
10	Determine the millivolt readings using the difference in readings between a standard and the unknowns.

3.6.2.1 Method of Calibration. The condition of the chloride selective-ion electrode, reference electrode, reference electrode filling solutions, and the presence of interfering substances such as bromide, iodide, fluoride, sulfide, cyanide, and hydroxide can cause deviations in the sample millivolt readings. The electrode response slope will remain constant. However, use of this method is based on the constant electrode response slope and the use of a titration for calibration. For the equation shown in the calculation section, the electrode response slope is -56 millivolts per decade (a ten-fold change in concentration).

Perform a silver nitrate titration as explained in Table 3.11 for use as a reference solution. This calibrating titration must be performed for each batch of sample. Perform the titration on a high concentration solution, i.e., a solution with a low initial millivolt reading.

3.6.2.2 Silver Nitrate Titration. This titration may be used for chloride analysis to determine the electrode response slope or for verification of other chloride concentrations. This method is the reference for the standard calibration method.

Table 3.11: Procedure for Silver Nitrate Titration

Step	Action
1	Pipet a 50 mL (1.7 oz.) sample into a clean, dry high-form electrolytic beaker.
2	Add three or four drops of methyl red indicator solution.
3	Acidify to a pale pink endpoint.
4	Prepare the electrodes for use by filling, cleaning, and drying them.
5	Immerse the electrodes in the sample solution, stir, and allow the millivolt readings to stabilize as above.
6	Record this initial millivolt reading (IMV) and start the titration by adding silver nitrate solution in 0.2 mL (0.0006 oz.) increments.
7	Allow the millivolt readings to stabilize after each addition.
8	Record the millivolt reading or change in millivolt reading between additions.
9	Determine the titration endpoint. The endpoint occurs at the greatest change in millivolt reading.

Table 3.12: Example of determination of titration endpoint

Titrant Volume (mL [oz.])	MV	Δ MV	Δ^2 MV
4.0 (0.135)	220.5	9.6	
4.2 (0.142)	230.1	16.2	+6.6
4.4 (0.149)	246.3	26.5	+10.3

4.6 (0.156)	272.8	22.7	-3.8
4.8 (0.162)	295.5	12.9	-9.8
5.0 (0.169)	308.4		

The endpoint is located where Δ^2MV equals zero. This may be determined graphically or by linear interpolation using one point on either side of zero as shown below:

<u>Volume (mL[oz.])</u>	<u>Δ^2MV</u>
4.4(0.149)	+10.3
4.6(0.156)	3.8

$$\Delta V = 0.2\text{mL}$$

$$\text{Endpoint} = 4.4 \text{ mL} + \frac{0.2 \text{ mL}}{10.3+3.8} = 4.4\text{mL}+0.146 \text{ mL} \quad (3-13)$$

$$\text{Endpoint} = 4.55 \text{ mL}$$

Accuracy of the method allows determination of the endpoint to the nearest 0.05 mL.

Calculation of the weight percent chloride in the concrete can be determined by:

$$\text{Wt.\% Chloride} = \frac{\text{Wt. Chloride}}{\text{Wt. Concrete}} \quad (3-14)$$

Where:

$$\text{Wt. Chloride} = (\text{Titrant volume})(\text{Titrant normality})(\text{Chloride molecular weight}) \\ (\text{Aliquot factor})$$

Where:

$$\text{Titrant Volume} = V(\text{mL})$$

$$\text{Titrant Normality} = N(\text{mol/L})$$

$$\text{Chloride Molecular Weight} = 35.453$$

$$\text{Aliquot factor} = 10$$

Wt. Concrete = 0 g

$$\text{Wt. \% Chloride} = \frac{(35.453)(10)\text{VN } 1000\text{mL } (100\%)}{30.00}$$

Wt. % Chloride = 1.182 VN %
ppm Chloride = 11820 VN
pounds/ton Chloride = 47.28 VN

This test method is from the TxDOT “*Manual of Testing Procedures, Volume III, Test Method Tex 617-J, September 1995.*”

The chloride powder test will be used in conjunction with the other tests presented in this thesis and tests that may develop between the time of this writing and the conclusion of the research project.

Chapter 3 presents the test development section of this thesis. Chapter 4 will present preliminary results that were obtained prior to completion of this thesis. These column models were designed to simulate the TxDOT typical column under severe exposure conditions. These conditions have been established on the basis of research and BRINSAP study conducted along the coastal districts, as well as districts above the de-icing line.

Chapter 4

Results and Discussion

4.1 Introduction. At the time of the writing of this thesis, the research team has gathered preliminary test results. These results will be presented in this section. The importance of these early results is not to gather conclusions, but rather to prepare for autopsy's of certain specimens and to check for possible flaws in the testing apparatus or the experiment itself.

At the time of this writing the specimens have been exposed for approximately 788 days. The matrix of variables is large and the evaluation of the data will be ongoing as the duration of the study progresses. The occurrence of corrosion and its proximity in relation to the rest of the column is an example of the types of variables presented as the study progresses in age. Some of the columns do not exhibit any signs of corrosion. Others are suggesting early signs. As mentioned in Chapter 3, the Half-Cell test coupled with chloride powder samples can yield meaningful results. The remainder of this section will deal with results received to date.

The study can change direction along its five-year path; therefore to report preliminary results with conclusions associated would be premature. With this understanding in mind, the experiment and the relevancy of the model itself can be examined. In addition, the preliminary results will be examined to “test” the author's hypothesis regarding capillary or wicking effect. The model, unlike the coastal columns, has no tidal action. However, the salt water is applied to one face. Therefore the location of the early half-cell tests have some merit.

4.2 Active Specimens. Appendix B contains graphic and tabulated figures of data

collected over 788 days worth of half-cell readings. Figure A.6 through A.10. illustrate the plotted values of a typical post-tensioned column specimen. Currently all ten of the specimens cast are active. Table 4.1 below gives an accounting of the specimens, and shows the current probability of corrosion occurring.

Table 4.1: Summary of the Ten Specimens Probability of Corrosion

Specimen Number	Probability of Corrosion
1 DJ-TC-N	>90 % Probability
2 PT-TC-N-PD	< 10 % Probability
3 NJ-TC-N	>10 % & < 90% Probability
4 DJ-TC-S	< 10 % Probability
5 PT-TC-S-PD	>10 % & < 90% Probability
6 NJ-TC-S	>90 % Probability
7 PT-TC-S-EB	>90 % Probability
8 PT-TC-S-GB	>90 % Probability
9 DJ-FA-S	>10 % & < 90% Probability
10 PT-FA-S-PD	>10 % & < 90% Probability

Table 4.1 has some interesting preliminary results. Notice the 35% by volume fly ash mixes all have less than a 90% chance of corrosion. This was expected as the permeability of the concrete matrix has the potential to be much denser than the TxDOT Class C mix design. This fact was illustrated in Chapter 3 in Section 3.3.1. Early results also indicate a slight advantage to the plastic duct that encompasses the post-tensioning reinforcement. As expected, the corrosion indications are greater near the bottom of the specimens as illustrated in several of the graphs shown in Appendix B.

The possibility that “wicking” is occurring in the specimens is indicated by the bars that have a greater than 90% possibility of corrosion that are clearly outside of the drip zone and above the water line. Consider Figure B.8B that illustrates the probability of corrosion in PT bars 1 and 2. While the corrosion in Bar 2 is expected due to the

direction of the moment and the orientation of the dripper location, the probability of corrosion is not expected in bar 3. The graph also indicates a wide range of scatter. This scatter suggests that hard conclusions can not be drawn at this time. Even the middle location of bar 2 has had high half-cell potential between the 150 to 300 day range. In addition to these results are the comparisons stated at the outset of this thesis as presented in Section 3.2.1.

4.3 Connection Comparisons. The connection types, without service load, are found in Column Specimens 1, 2 and 3. Without service load or moment, the only connection that has yet to exhibit any signs of corrosion is the post-tensioned column connection. The doveled connection is already in the “greater than 90% probability of corrosion”. The doveled connection construction process allows for the possibility of a slight crack between the column and the foundation. This potential “flaw” allows for the migration of chloride ions into the column. Post-tensioning provides the opportunity to “seal” the joint with PT force. The “no joint” case is expected to yield little corrosion from the joint because of the cover provided around the conventional reinforcement.

Columns 4, 5 and 6 are the same case as above but with the addition of service load applied. The preliminary results differ slightly, in the fact that the doveled joint has not exhibited any signs of corrosion. This phenomenon can be attributed to the fact that the service load acts like the post-tensioning in “sealing” the interface between the foundation and the column. Column 5 is very similar in behavior to Column 2, where as expected there is little corrosion indicated from the preliminary half-cell readings. The “no joint” case’s behavior is irregular. This joint has a high probability of corrosion. This possibility would not be expected due in part to the construction of the joint. As in the case with many of the specimens, the possibility of corrosion can be attributed to many factors, several of which are not related to the joint construction.

4.4 Effects of The Concrete. As mentioned earlier, the Column specimens 9 and 10 are

comprised of a concrete matrix, which contains 35% percent flyash. The preliminary results indicate that this concrete's performance is generally better than the TxDOT class C concrete. A closer evaluation of the equal comparisons i.e. Column 9 with Column 4 and Column 10 with Column 5 reveal a slight edge in the performance of the TxDOT Class C concrete over the 35% flyash.

4.5 Effects of PT Protection. The bar protection includes both epoxy coated bar and galvanized bar in Column Specimens 7 and 8 respectively. Currently the protected bars are not performing as well as the non-coated bar in the same environment. In Column Specimen 5 the half-cell readings are very closely aligned for 3 of the four bars. In contrast is Column Specimen 7, where bars 1 and 2 are exhibiting strong possibilities of corrosion. This comparison directly compares epoxy and galvanized bar alongside of the conventional black bar. Note that the single unique variable in Column Specimen 7, beyond the bars, is the duct. Ducts 1 and 2 contain epoxy and galvanized bar and are comprised of plastic. Ducts 3 and 4 are galvanized steel ducts with black bar.

In Column Specimen 8, the bar and duct combinations are similar to Column Specimen 7. The difference between Columns 7 and 8 lies in the galvanized bar in lieu of epoxy bar. The early results indicate a stronger resistance to corrosion. The graph in Appendix B, Figure B.8B illustrates the PT bar's half-cell potential. Note that the bar readings and behavior are very close and quite near the demarcation of a greater than 90% chance of corrosion. As with earlier comparisons of other variables, the scatter in the data and only one test make it impossible to draw firm conclusions.

4.6 Effects of the Duct Material. In each of the PT Column Specimens the configuration of duct is two plastic ducts in locations 1 and 2 and two galvanized ducts in locations 3 and 4. In general, the comparison of all the columns does not present a clear favorite. The even potential of the duct comparisons is best illustrated in Column Specimen 2 where the potential readings for all four bars are very close. In Column

Specimen 5 the plastic duct in location 1 seems to be performing with less potential than the rest of the locations. Column Specimen 7 has plastic duct in conjunction with epoxy coated bar. Further evaluation is required to determine if the potential corrosion stems from the bar or duct. The galvanized bar and PT bar behavior in Column Specimen 8 is very uniform with little corrosion potential exhibited. The bar and duct potential readings are very close to the same potential. The fly ash Column Specimen, number 10, has some variability between duct material. This potential difference can be seen in Appendix B in Figure B.10. where locations 2, 3 and 4 have a +50mV greater potential than location 1. As always, several possibilities exist for this behavior and the research teams future studies will try to pin point the impact of the duct with several tests in the future.

The early results from the half-cell survey are a good indication that the experiment and especially the models, have the potential to yield meaningful results. The research team intends to take several chloride powder samples and some bore scope tests. Finally, several of the specimens will be autopsied at the conclusion of the test period. At the time of this thesis the indications are favorable that the models will give meaningful results that are accurate and reflect the actual corrosion mechanism that occurs in Texas bridge columns today.

Chapter 5

Summary, Conclusions and Recommendations

Corrosion of substructure components is a multi-billion dollar expense in the United States. This problem is comparably expensive in Texas. Currently the replacement value of Texas Bridges, damaged from substructure corrosion in one of the twenty-five districts, is estimated at \$100 million and statewide is estimated to be \$2.2 billion. In order to improve the substructures in Texas bridges, it must be accepted that the problem exists and that enhancement of protection schemes in areas of severe corrosion environment need to be improved.

In light of this information, the main objectives of this thesis were to:

- a.) Define the reinforced concrete substructure problem in Texas with “on-system” bridges, including and focusing on Districts where corrosion is likely and the exposure conditions are severe. Refining that focus by defining areas of the substructure under durability attack.

- b.) Construct a model of current Texas bridge columns that are conventionally reinforced and post-tensioned. Replicate the loading and exposure conditions that the actual columns are currently subjected to and design model columns with various protection schemes to enhance durability of the substructure element. Paramount among the protection schemes is the application of post-tensioning to reduce potential crack width, increase cover, and enhance the elements defense against corrosion.

At the time of this thesis TxDOT is currently developing a regional specification for their use with de-icing and anti-icing chemicals. Several of the Districts have adopted these new de-icing chemicals. Paramount among those chemicals is magnesium

chloride, which may prove to be more corrosive than conventional rock salt. As the state's bridges continue to exist in a corrosive environment, new protection schemes will need to be developed. This thesis attempts to address some of these issues. The conclusions of this thesis can be summarized as follows:

- The corrosion of current Texas bridge substructures and the replacement of these structures was a cost that exceeds a billion dollars.
- Currently 8% of the "on-system bridges in Texas have a BRINSAP substructure rating of 5 or below.
- Bridge substructures can and have controlled the bridges life cycle.
- The durability attacks are reducing the design life of bridges, where substructure durability controls, by nearly half of the TxDOT design life.
- A realistic test specimen and exposure simulation was developed.
- The designed 3/5 scale model specimens reasonably reflect the behavior of current TxDOT bridge columns at this time.
- Further BRINSAP information is required to measure the extent of durability attack and the effectiveness to protection measures so that TxDOT can maximize the design of substructure components subject to severe exposure.

The major conclusion of this study to date, is the fact that there is a durability concern with Texas Bridge substructures. The ultimate solution or even recommendations to elevate this problem are still years away as the research program, Project 1405, is a long term study. The author hopes that the models may yet lend a part in the eventual protection scheme for Texas bridge columns.

Appendix A
Preliminary Half-Cell Results
for
Column Specimens

Figure A.2: Half-Cell Potentials for Df-TC-S (22)

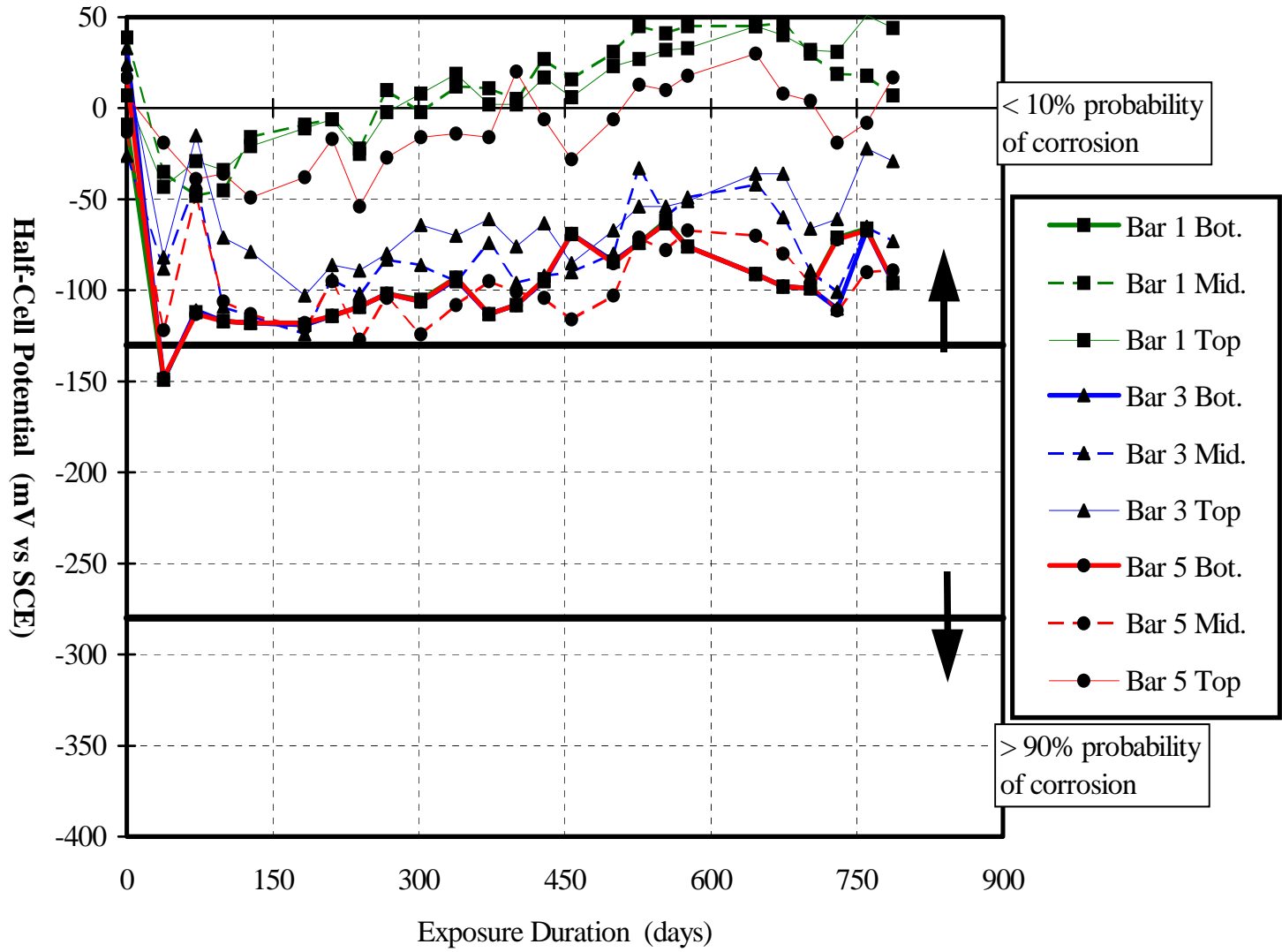
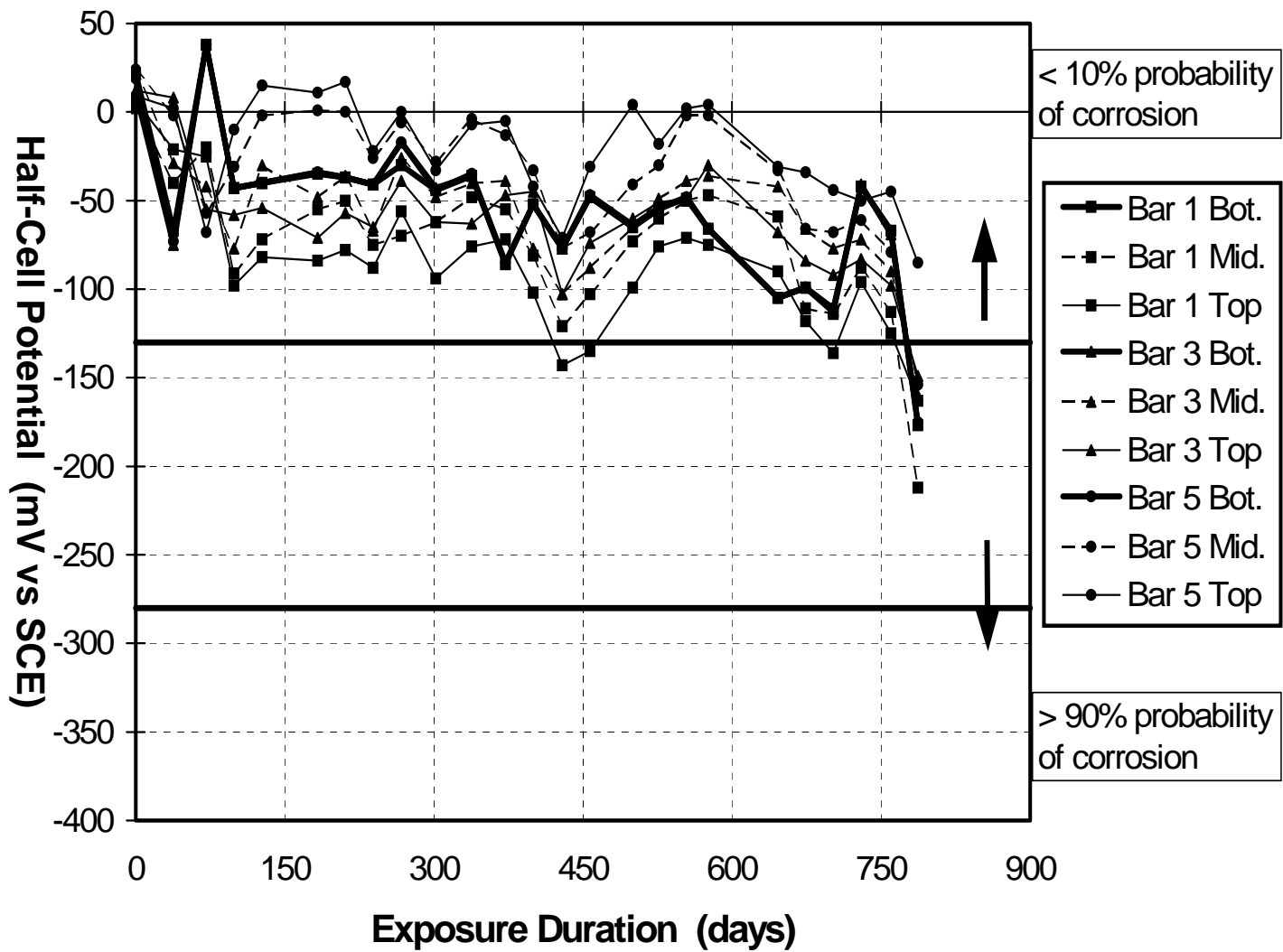


Figure A.5: Half-Cell Potential for NJ-TC-N (22)



Bibliography

1. **T.Y. Lin and F. Kulka**, “Fifty-Year Advancement in Concrete Bridge Construction”, *J.Const. Div.*, American Society of Civil Engineers, September 1975, pp.491-510.
2. **Collins, M. P. and Mitchell, D.**, Prestressed Concrete Basics, Canadian Prestressed Concrete International, Ottawa, Ontario, Canada, 1987.
3. **Hamilton, R.H.**, ”Investigation of Corrosion Protection Systems for Bridge Stay Cables”, *PhD. Dissertation*, The University of Texas at Austin, December 1995.
4. **Whiting, D. and Mitchell, T.**, “ History of the Rapid Chloride Permeability Test,” *Transportation Research Record* No. 1335, Jan. 1992.
5. **Tia, M. and Bloomquist, D. and Yang, M. and Meletiou, C. and Amornsivilai, P. and Shih, C. and Bobson, E. and Richardson, D.**, “Extensive Study of Field and Laboratory Study of Modulus of Rupture and Permeability of Structural Concrete in Florida for the Development of a Concrete Performance Specification, “ College of Engineering at the University of Florida, Gainesville, 1992.
6. **Fontana, M. G.**, Corrosion Engineering 3rd Edition, McGraw-Hill, Inc., 1986.
7. **American Concrete Institute**, “Building Code Requirements for Reinforced Concrete and Commentary”, ACI-318-89, Detroit; 1989.
8. **ACI Committee 224**, “Control of Cracking in Concrete Structures,”(ACI224.1R-93), American Concrete Institute, Detroit, MI,1990.
9. **Texas Department of Transportation**, “Specifications for the Construction and Maintenance of Highways, Streets and Bridges”, 1993
10. **American Association of State Highway and Transportation Officials**, “Standard Specifications for Highway Bridges, Sixteenth Edition”, American Association of State Highway and Transportation Officials, Washington, D.C., 1996.

11. **American Society of Testing and Materials**, “Standard Test Method for Half-Cell Potentials of Uncoated Reinforcing Steel in Concrete.” ASTM Designation: C-876, Philadelphia, American Society for Testing and Materials, 1991
12. **Freytag, G.**, “Development of a Field Corrosion Detection and Monitoring Program for Reinforced Concrete Bridges”, MS Thesis, The University of Texas at Austin, May 1994.
13. **Jones, D. A.**, Principles and Prevention of Corrosion. New York: Macmillan Publishing Co., 1992
14. **Bridge Inventory, Inspection and Appraisal Program (BRINSAP) Manual of Procedures**, State Department of Highways and Public Transportation, 1984.
15. **Cox, R.**, Director of Bridge Construction, Texas Department of Transportation: November 20, 1996. Personal Interview.
16. **Mirsa, S. and Uotomo, T.**, “Behavior of Concrete Beams and Columns in Marine Environment When Corrosion of Reinforcing Bars Takes Place,” Durability of Concrete, Second International Conference, ACI SP 106, pp. 127-146.
17. **American Society of Testing and Materials**, “Standard Test Method for Half-Cell Potentials of Uncoated Reinforcing Steel in Concrete.” ASTM Designation: C-876, Philadelphia, American Society for Testing and Materials, 1991
18. **Burns, Ned H. and T.Y. Lin**, Design of Prestressed Concrete Structures, New York. John Wiley & Sons, 1981.
19. **Lynch, M.**, State of Texas BRINSAP Coordinator, Texas Department of Transportation: September, 1996. Personal Interview.
20. **Bonstedt, H.O.**, “Specifically Wrong—But Generally Right! Actuarial Life Expectancy Projections for Bridges”, *ACI Spring Convention*, American Concrete Institute, 1996.

21. **Federal Highway Administration**, "Impedance Spectroscopy for the Evaluation of Corrosion Inhibitors in Highway Deicers" Publication No. FHWA-RD-96-178, March 1997.
22. **West, J.S.**, "Durability Design of Post-Tensioned Bridge Substructures", Doctor of Philosophy Dissertation, The University of Texas at Austin, May, 1999.
23. **American Society of Testing and Materials**, "Standard Test for Electrical Indication of Concrete's Ability to Resist Chloride Ion Penetration," ASTM C1202-97, Philadelphia, PA, 1997.
24. **Koester, Bradley D.**, "Evaluation of Cement Grouts for Strand Protection Using Accelerated Corrosion Tests," Master Of Science Thesis, The University of Texas at Austin, December 1995.
25. **Schokker, Andrea J.**, "Improving Corrosion Resistance of Post-Tensioned Substructures Emphasizing High Performance Grouts," Doctor of Philosophy Dissertation, The University of Texas at Austin, May, 1999.